View metadata, citation and similar papers at core.ac.uk

brought to you by CORE

provided by NASA Technical Reports Server

24P mif

X-582-73-37

PREPRINT

NASA TM X- 70620

FILTERING THEORY APPLIED TO ORBIT DETERMINATION

VICENTE TORROGLOSA

N74-21

(NASA-TM-X-70620) FILTERING THEORY APPLIED TO ORBIT DETERMINATION (NASA) 69 p HC $6.25 CSCL 22C

G3/30 Unclas 36510

DECEMBER 1973

GSFC

GODDARD SPACE FLIGHT CENTER

GREENBELT, MARYLAND

For information concerning availability
of this document contact:

Technical Information Division, Code 250
Goddard Space Flight Center
Greenbelt, Maryland 20771

(Telephone 301-982-4488)

X-582-73-379

FILTERING THEORY APPLIED TO ORBIT DETERMINATION

Vicente Torroglosa
INTA-ESRO*

December 1973

*Work performed under ESRO Applied Research Contract No. 341/71/AR.

GODDARD SPACE FLIGHT CENTER
Greenbelt, Maryland

FILTERING THEORY APPLIED TO ORBIT DETERMINATION

Vicente Torroglosa

ABSTRACT

Modifications to the extended Kalman filter and the Jazwinski filter are made and compared with the classical extended Kalman filter in applications to orbit determination using real data. The results obtained in this study show that with the kind of data available today, the application of filtering theories in this field presents many problems.

Preceding page blank

CONTENTS

PRECEDING PAGE BLANK NOT FILMED

LIST OF FIGURES

Notes: 1) The different initial covariance matrices for the different satellites may be seen in Tables 1, 2 and 3.

* The influence of this parameter is being studied.

FILTERING THEORY APPLIED TO ORBIT DETERMINATION

INTRODUCTION

After more than a decade of working with estimation theories and their possible applications, no definitive conclusions had been obtained about whether or not a filter can be used successfully in the orbit determination field.

To date most of the studies in this area have dealt with simulated data, and the conclusions which have been reached are as follows:

1. The extended Kalman filter may be used successfully in the orbit determination problem for short lengths of time, i.e., short arc lengths.

2. For applications to longer spans of time, this filter should be modified to avoid divergence. This problem occurs because of the lack of knowledge of the dynamic system as well as the linearization of the original problem. The adaptive filter seems to be the solution to this problem.

This study is an attempt to find a way of applying such estimation theories to real world orbit determination problems.

I

EXTENDED KALMAN FILTER

Suppose that the equation of motion is described by the following nonlinear stochastic differential equation

$$\begin{aligned} dx_\tau &= f(x_\tau, \tau)\, d\tau + G(\tau)\, d\beta_\tau, \quad \tau \geq 0 \\ x_0 &\sim N(\hat{x}_0, P_0) \end{aligned} \tag{1-1}$$

formally equivalent to:

$$\begin{aligned} &E[x_0] = \hat{x}_0, \\ &E[(x_0 - \hat{x}_0)(x_0 - \hat{x}_0)^T] = P_0 \\ &\frac{dx_\tau}{d\tau} = f(x_\tau, \tau) + G(\tau)\, u_\tau \end{aligned} \tag{1-2}$$

Where:

x_τ, the $n \times 1$ state vector

$f(x_\tau, \tau)$ $n \times 1$ continuous function vector

$G(\tau)$, $n \times r$ continuous function matrix

$\{\beta_\tau, \tau \geq 0\}$, $r \times 1$ Brownian motion process

$(E\{d\beta_\tau\, d\beta_\tau^T\} = Q(\tau)\, d\tau)$

$\{u_\tau, \tau \geq 0\}$, $r \times 1$ White gaussian vector process

$(u_\tau \sim N(0, Q(\tau))$, i.e., $E[u_\tau] = 0$, $E[u_\tau u_\tau^T] = Q(\tau)$

The discrete nonlinear observations can be expressed as

$$\begin{aligned} y_K &= h(x_K) + v_K, \\ v_K &\sim N(0, \sigma^2{}_K). \end{aligned} \tag{1-3}$$

(These observations are taken at time instants t_K and $\tau = t - t_{K-1}$, $(\tau_K = t_K - t_{K-1})$.

Suppose that we generate a reference deterministic trajectory $\bar{x}_\tau$, satisfying

$$\frac{d\bar{x}_\tau}{d\tau} = f(\bar{x}_\tau, \tau), \tau \geqslant 0. \tag{1-4}$$

Define at each point in time

$$\delta x_\tau = x_\tau - \bar{x}_\tau \tag{1-5}$$

which satisfies the equation

$$\frac{d(\delta x_\tau)}{d\tau} = f(x_\tau, \tau) - f(\bar{x}_\tau, \tau) + G(\tau) u_\tau$$
$$\delta x_0 \sim N(\hat{x}_0 - \bar{x}_0, P_0) \tag{1-6}$$

If the deviations (δx) from the reference trajectory are small, a Taylor series expansion gives

$$\frac{d(\delta x_\tau)}{d\tau} = f_x(\bar{x}_\tau, \tau)\, \delta x_\tau + G(\tau) u_\tau \tag{1-7}$$

where $f_x(x_\tau, \tau)$ is a function of time only, i.e., (1-7) is a linear system.

Defining the nominal measurement as

$$\bar{y}_K = h(\bar{x}_K), (x_K = \bar{x}_{\tau_K}), \tag{1-8}$$

then

$$\delta y_K = y_K - \bar{y}_K = h_x(\bar{x}_K)\, \delta x_K + V_K, (\delta x_K = \delta x_{\tau_K}). \tag{1-9}$$

Equation (1-7) can be discretized as

$$\delta x_K = \Phi(t_K, t_{K-1})\, \delta x_{K-1} + \omega_K \tag{1-10}$$

where Φ, the state transition matrix, is defined as:

$$\frac{d\Phi(t, t_{K-1})}{dt} = f_x(\bar{x}_\tau, \tau)\,\Phi(t, t_{K-1}) \tag{1-11}$$

with

$$\Phi(t_{K-1}, t_{K-1}) = I, \qquad \tau = t - t_{K-1} \tag{1-12}$$

and $\omega_K \sim N(0, Q_K)$, where

$$Q_K = \int_{t_K}^{t_{K+1}} \Phi(t_K, s)\,G(s)\,Q(s)\,G^T(s)\,\Phi^T(t_K, s)\,ds \tag{1-13}$$

where

$$\Phi(t_K, s) = \Phi(t_K, t_{K-1})\,\Phi(t_{K-1}, s) \tag{1-14}$$

and

$$\Phi(t_{K-1}, s) = \Phi^{-1}(s, t_{K-1}). \tag{1-15}$$

Now the linear filter is directly applicable to the linearized system (1-9 and 1-10) and the equations for $\delta\hat{x}$ and P are as follows:

a. Prediction:

$$\delta\hat{x}_{K/K-1} = \Phi(t_K, t_{K-1})\,\delta\hat{x}_{K-1/K-1} \tag{1-16}$$

$$P_{K/K-1} = \Phi(t_K, t_{K-1})\,P\,\Phi^T(t_K, t_{K-1}) + Q_K \tag{1-17}$$

b. Update:

$$\delta\hat{x}_{K/K} = \delta\hat{x}_{K/K-1} + K_{t_K}\left[\delta y_K - h_x(\bar{x}_K)\,\delta\hat{x}_{K/K-1}\right] \tag{1-18}$$

$$P_{K/K} = \left[I - K_{t_K}\ h_x(\bar{x}_K)\right]P_{K/K-1}\left[I - K_{t_K}\ h_x(x_K)\right]^T + K_{t_K}\,\sigma_K{}^2\,K^T{}_{t_K} \tag{1-19}$$

The Kalman gain is

$$K_{t_K} = P_{K/K-1}\,h_x{}^T(\bar{x}_K)\quad\left[h_x(\bar{x}_K)\,P_{K/K-1}\,h_x{}^T(\bar{x}_K) + \sigma_K{}^2\right]. \tag{1-20}$$

If the reference trajectory is chosen such that

$$\bar{x}(0) = \hat{x}_{K-1/K-1} \tag{1-21}$$

we have from (1-5)

$$\delta\hat{x}_{K-1/K-1} = E\left\{x_{K-1/K-1} - \hat{x}_{K-1/K-1}\right\} = 0 \tag{1-22}$$

then from (1-16)

$$\delta\hat{x}_{K/K-1} = 0 \tag{1-23}$$

and

$$\begin{aligned}\hat{x}_{K/K-1} &= E\left\{x_{K/K-1}\right\} = E\left\{\delta x_{K/K-1} + \bar{x}_{K/K-1}\right\} \\ &= \bar{x}_{K/K-1}.\end{aligned} \tag{1-24}$$

In the same way

$$P_{K/K-1} = E\left\{(x_{K/K-1} - \hat{x}_{K/K-1})(x_{K/K-1} - \hat{x}_{K/K-1})^T\right\} = E\left\{(\delta x_{K/K-1})(\delta \tilde{x}^T_{K/K-1})\right\} \tag{1-25}$$

and

$$E\left\{(x_{K/K} - \hat{x}_{K/K})(x_{K/K} - \hat{x}_{K/K})^T\right\} = P_{K/K} = E\left\{(\delta x_{K/K}\ \delta x^T_{K/K})\right\}. \tag{1-26}$$

Now we may state the evolution of the mean and the covariance matrix of the state for the extended Kalman filter:

a. Prediction:

$\hat{x}_{K/K-1}$ is obtained from

$$\frac{d\hat{x}_\tau}{d\tau} = f(\hat{x}_\tau, \tau) \tag{1-27}$$

with

$$\hat{x}_0 = \hat{x}_{K-1/K-1} \tag{1-28}$$

for

$$\tau = \tau_K = t_K - t_{K-1} \tag{1-29}$$

$$P_{K/K-1} = \Phi(t_K, t_{K-1})\, P_{K-1/K-1}\, \Phi^T(t_K, t_{K-1}) + Q_K \tag{1-30}$$

b. Update:

$$\hat{x}_{K/K} = \hat{x}_{K/K-1} + K_{t_K}\left[Y_K - h(\hat{x}_{K/K-1})\right] \tag{1-31}$$

The equations (1-19) and (1-20) remain unchanged.

II

JAZWINSKI FILTER

In the orbit determination problem the equations of motion may be stated as follows:

$$\frac{dV}{dt} = f_1(R, V, \tau) + f_2(R, V, \tau) + G(\tau)\, u_\tau \tag{2-1}$$

$$\frac{dR}{dt} = V \tag{2-2}$$

where:

f_1, includes the accelerations that are well known

f_2, possible unknown accelerations and the errors in f_1.

On short lengths of time, f_2 can be taken as:

$$f_2 = f_{2(\tau=0)} + \frac{df_2}{dt}_{(\tau=0)} \tau. \tag{2-3}$$

If

$$u = f_{2(\tau=0)} \tag{2-4}$$

$$\dot{u} = \frac{df_2}{dt}_{(\tau=0)} \tag{2-5}$$

then the equation (2-1) becomes:

$$\frac{dV}{dt} = f_1(R, V, \tau) + u + \dot{u}\tau \tag{2-6}$$

if the state noise is not included.

The lack of knowledge of u and $\dot{u}$ makes it necessary to include these in the state and estimate them as well as the usual state vector (position R and velocity V).

Now we may state the complete dynamical system

$$\frac{dR}{d\tau} = V \tag{2-7}$$

$$\frac{dV}{d\tau} = f_1(R, V, \tau) + u + \dot{u}\tau \tag{2-8}$$

$$\frac{du}{d\tau} = \dot{u} \tag{2-9}$$

$$\frac{d\dot{u}}{d\tau} = 0 \tag{2-10}$$

The initial conditions for $\tau = 0$, ($t = t_{K-1}$), are

$$E\left\{R^T : V^T\right\} = E\left\{x^T\right\} = \hat{x}^T_{K-1} \tag{2-11}$$

$$E\left\{u\right\} = \hat{u}_{K-1} \tag{2-12}$$

$$E\left\{\dot{u}\right\} = \hat{\dot{u}}_{K-1} \tag{2-13}$$

$$E\left\{(x - \hat{x})(x - \hat{x})^T\right\} = P_{K-1/K-1} \tag{2-14}$$

$$E\left\{(x - \hat{x})(u - \hat{u})^T\right\} = C_{u_{K-1/K-1}} \tag{2-15}$$

$$E\left\{(x - \hat{x})(\dot{u} - \hat{\dot{u}})^T\right\} = C_{\dot{u}_{K-1/K-1}} \tag{2-16}$$

$$E\left\{(u - \hat{u})(u - \hat{u})^T\right\} = U_{uu_{K-1/K-1}} \tag{2-17}$$

$$E\left\{\left(u - \hat{u}\right)\left(\dot{u} - \dot{\hat{u}}\right)^T\right\} = U_{u\dot{u}_{K-1/K-1}} \tag{2-18}$$

$$E\left\{\left(\dot{u} - \dot{\hat{u}}\right)\left(\dot{u} - \dot{\hat{u}}\right)^T\right\} = U_{\dot{u}\dot{u}_{K-1/K-1}} \tag{2-19}$$

and the measurement model is

$$y_K = h\left(x_K, \tau_K\right) + v_K, \quad t = t_K \tag{2-20}$$

where τ_K is a zero mean, white, gaussian noise sequence with

$$E\left\{v_K \quad v_K{}^T\right\} = R_K \tag{2-21}$$

The predictions for the estimate of the state $\left(\hat{x}_{K/K-1}, \hat{u}_{K/K-1}, \dot{\hat{u}}_{K/K-1}\right)$ and the estimate of the state covariance matrix for $t = t_K$, $\left(\tau = \tau_K = t_K - t_{K-1}\right)$ are:

$$\hat{x}_{K/K-1} = F(\hat{x}_{K-1/K-1}, \hat{u}_{K-1/K-1}, \dot{\hat{u}}_{K/K-1}, \tau_K) \tag{2-22}$$

$$\hat{u}_{K/K-1} = \hat{u}_{K-1} + \tau_K \dot{\hat{u}}_{K/K-1} \tag{2-23}$$

$$\dot{\hat{u}}_{K/K-1} = \dot{\hat{u}}_{K-1/K-1} \tag{2-24}$$

$$\begin{aligned} P_{K/K-1} = {} & \Phi P_{K-1/K-1} \Phi^T + \Phi C_{u_{K-1/K-1}} \psi^T + \psi C^T{}_{u_{K-1/K-1}} \Phi^T \\ & + \psi U^T{}_{u\dot{u}_{K-1/K-1}} \psi^T + \Phi C_{\dot{u}_{K-1/K-1}} \psi d^T + \psi d\, C^T{}_{\dot{u}_{K-1/K-1}} \Phi^T \\ & + \psi U_{u\dot{u}_{K-1/K-1}} \psi d^T + \psi d\, U^T{}_{u\dot{u}_{K-1/K-1}} \psi^T + \psi d\, U_{\dot{u}\dot{u}_{K-1/K-1}} \psi d^T \end{aligned} \tag{2-25}$$

$$\begin{aligned} C_{u_{K/K-1}} = {} & \Phi C_{u_{K-1/K-1}} + \psi U_{uu_{K-1/K-1}} \\ & + \tau_K \left(\Phi C_{\dot{u}_{K-1/K-1}} + \psi U_{u\dot{u}_{K-1/K-1}} + \psi_d U_{\dot{u}\dot{u}_{K-1/K-1}}\right) \end{aligned} \tag{2-26}$$

$$C\dot{u}_{K/K-1} = \Phi\, C\dot{u}_{K-1/K-1} + \psi\, U_{u\dot{u}K-1/K-1} + \psi d\, U_{\dot{u}\dot{u}K-1/K-1} \tag{2-27}$$

$$U_{uuK/K-1} = U_{uuK-1/K-1} + \tau_K \left(U_{u\dot{u}K-1/K-1} + U^T{}_{u\dot{u}K-1/K-1} + \tau_K\, U_{\dot{u}\dot{u}K-1/K-1} \right) \tag{2-28}$$

$$U_{u\dot{u}K/K-1} = U_{u\dot{u}K-1/K-1} + \tau_K\, U_{\dot{u}\dot{u}K-1/K-1} \tag{2-29}$$

$$U_{\dot{u}\dot{u}K/K-1} = U_{\dot{u}\dot{u}K-1/K-1} \tag{2-30}$$

where:

$$\Phi = \Phi_{K/K-1} = \left[\frac{\partial \hat{x}_K}{\partial \hat{x}_{K-1}} \right] \tag{2-31}$$

$$\psi = \psi_{K/K-1} = \left[\frac{\partial \hat{x}_K}{\partial \hat{u}_{K-1}} \right] = \begin{bmatrix} \frac{\tau_K^2}{2} & 1 \\ \tau_K & 1 \end{bmatrix} \tag{2-32}$$

$$\psi d = \psi d_{K/K-1} = \left[\frac{\partial \hat{x}_K}{\partial \hat{u}_{K-1}} \right] = \begin{bmatrix} \frac{\tau_K^2}{6} & 1 \\ \frac{\tau_K^2}{2} & 1 \end{bmatrix} \tag{2-33}$$

Φ is the state transition matrix and I, 3 X 3, Identity matrix.

The update at observation K is:

$$\hat{x}_{K/K} = \hat{x}_{K/K-1} + K_x \left[y_K - h\left(\hat{x}_{K/K-1} \tau_K \right) \right] \tag{2-34}$$

$$\hat{u}_{K/K} = \hat{u}_{K/K-1} + K_u \left[y_K - h\left(\hat{x}_{K/K-1}, \tau_K \right) \right] \tag{2-35}$$

$$\hat{\dot{u}}_{K/K} = \hat{\dot{u}}_{K/K-1} + K_{\dot{u}} \left[y_K - h\left(\hat{x}_{K/K-1}, \tau_K \right) \right] \tag{2-36}$$

$$P_{K/K} = P_{K/K-1} - K_x\, h_x\, P_{K/K-1} \tag{2-37}$$

$$C_{u_{K/K}} = C_{u_{K/K-1}} - K_x\, h_x\, C_{u_{K/K-1}} \tag{2-38}$$

$$C_{\dot{u}_{K/K}} = C_{\dot{u}_{K/K-1}} - K_x\, h_x\, C_{\dot{u}_{K/K-1}} \tag{2-39}$$

$$U_{uu_{K/K}} = U_{uu_{K/K-1}} - K_u\, h_x\, C_{u_{K/K-1}} \tag{2-40}$$

$$U_{\dot{u}\dot{u}_{K/K}} = U_{\dot{u}\dot{u}_{K/K-1}} - K_u\, h_x\, C_{\dot{u}_{K/K-1}} \tag{2-41}$$

$$U_{\dot{u}\dot{u}_{K/K}} = U_{\dot{u}\dot{u}_{K/K-1}} - K_{\dot{u}}\, h_x\, C_{\dot{u}_{K/K-1}} \tag{2-42}$$

where:

$$h_x = h_{x_K} = \left[\frac{\partial h}{\partial x}\right] x = \hat{x}_{K/K-1}, \tau = \tau_K \tag{2-43}$$

$$K_x = K_{x_K} = P_{K/K-1}\, h^T{}_x,\, Y^{-1}{}_K \tag{2-44}$$

$$K_u = K_{u_K} = C^T u_{K/K-1}\, h^T{}_x\, Y^{-1}{}_K \tag{2-45}$$

$$K_{\dot{u}} = K_{\dot{u}_K} = C^T \dot{u}_{K/K-1}\, h^T{}_x\, Y^{-1}{}_K \tag{2-46}$$

$$Y_K = h_x\, P_{K/K-1}\, h^T{}_x + R_K \tag{2-47}$$

The following initial conditions are to be specified

$$\hat{x}_{0/0}, P_{0/0}, U_{uu_{0/0}}, U_{\dot{u}\dot{u}_{0/0}} \tag{2-48}$$

whereas

$$\hat{u}_{0/0}, \hat{\dot{u}}_{0/0} \tag{2-49}$$

are externally set to zero for lack of better information.

The inclusion of Equation (2-42) is the main difference between the filter described here and that of Reference 1. This inclusion avoids the covariance matrix of the state from becoming non-positive definite.

III

MODIFICATIONS

Several modifications have been made to the previous filters in an attempt tp solve some problems associated with their performance.

The main problem related to the EKF is the modeling of state noise. The assumption of white gaussian noise seems to be poor. But if we accept this assumption, we must still assign proper values for the variance.

On the other hand, the errors of modeling the dynamical system should be taken into account to avoid the filter divergence. The optimistic performance of the EKF without state noise leads to a growing difference between the actual state and the estimated state not reflected in the covariance matrix which continues to decrease as more observations are given. The filter divergence manifests itself in a secular growth of the predicted residuals which become clearly biased.

In an attempt to avoid the divergence in the EKF, while maintaining its simplicity, a modification has been made in the definition of the Kalman gain. This modified filter is going to be called MEKF.

The definition for the Kalman gain in the MEKF is

$$K_M(t_K) = K(t_K)\,(1 + Q_K) \tag{3-1}$$

where:

$$Q_K = \frac{n-1}{n}\,Q_{K-1} + \frac{1}{n}\,Q'_r \tag{3-2}$$

and

$$Q'_r = \begin{cases} \frac{1}{\sigma_K}\,\Sigma_r\,, & \text{if } \Sigma_r\left[y_K - h(\hat{x}_{K/K-1})\right] < 0 \\ 0\,, & \text{otherwise} \end{cases} \tag{3-3}$$

where:

$$\Sigma_r = \frac{n-1}{n}\,\Sigma_{r-1} + \frac{1}{n}\left[y_K - h(\hat{x}_{K/K-1})\right] \tag{3-4}$$

and K_{t_K} is given in (1-20). Σ is different for each observation type and station, and $\Sigma_0 = 0$.

This modification tries to avoid the increase in the mean of the residuals which are the main manifestation of the divergence. In this way the direction is kept but its magnitude is modified to avoid the filter divergence.

The third filter tested in this study has been a modification of the Jazwinski Filter described in Chapter II.

This filter is going to be called MJF and tries to make the JF adaptive.

The Jazwinski Filter shows great sensitivity to the values assigned to the initial covariances of u and $\dot{u}$. It seems desirable to have the ability to set these values correctly and automatically.

The covariance matrix of $\dot{u}$ can be used to regulate the process, so that the residuals are consistent with their statistics.

Assume that in each step we know $U_{\dot{u}\dot{u}}$ except for a factor. That is, if $U_{\dot{u}\dot{u}}$ is the covariance matrix given in the process described in Chapter II, the actual covariance matrix, $U'_{\dot{u}\dot{u}}$, is going to be:

$$U'_{\dot{u}\dot{u}_{K-1/K-1}} = (1 + q_{t_k})U_{\dot{u}\dot{u}_{K-1/K-1}} \tag{3-5}$$

and the covariance matrix of the state is

$$P'_{K/K-1} = P_{K/K-1} + q_K\,\Psi_d U_{\dot{u}\dot{u}}\,\Psi_d^T.$$

We now define

$$\Sigma_r = \frac{n-1}{n}\,\Sigma_{r-1} + \frac{1}{n}\,\frac{\left[y_K - h(\hat{x}_{K/K-1})\right]^2}{\left[h_x\, P_{K/K-1}\, h_x{}^T + \sigma_K\right]} \qquad (3\text{-}6)$$

Then

$$(h_x\, P_{K/K-1}\, h_x{}^T + \sigma_K)\,\Sigma_r = E\{r_K\}^2 \qquad (3\text{-}7)$$

where

$$\bar{r}_K^{\,2} = \left[y_K - h(\hat{x}_{K/K-1})\right]^2 \qquad (3\text{-}8)$$

and

$$E\left\{\bar{r}_K^{\,2}\right\} = h_x\, P_{K/K-1}\, h_x{}^T + \sigma_K + q'_K\; h_x \Psi_d\, P\, \Psi_d{}^T h_x{}^T \qquad (3\text{-}9)$$

$$q'_K = \begin{cases} \dfrac{(q_r - 1)\,(h_x\, P_{K/K-1}\, h_x{}^T + \sigma_K)}{h_x\, \psi_d\, P\, \psi_d{}^T\, h_x^T} & \text{, if positive} \\ 0 & \text{, otherwise} \end{cases} \qquad (3\text{-}10)$$

$$q_K = \frac{n-1}{n}\, q_{K-1} + \frac{1}{n}\, q'_K \,. \qquad (3\text{-}11)$$

To avoid the accumulating corrections in successive observations, after setting the new value $\dot{u}_{\dot{u}\dot{u}}$, q_K is reset to

$$q_K = \begin{cases} 1 - \dfrac{n-1}{n} \cdot \dfrac{1}{n}\left[\dfrac{1 + q'_K}{1 + q_K}\right] & \text{, if positive} \\ 0 & \text{, otherwise} \end{cases} \qquad (3\text{-}12)$$

A further step to completely automate the process would be the initialization of U_{uu} and $U_{\dot{u}\dot{u}}$. In the filter tested in this paper this is done by setting

$$U_{uu_{0/0}} = K f_{1_x} P_{0/0} f_{1_x}^T \tag{3-13}$$

$$U_{\dot{u}\dot{u}_{0/0}} = K \frac{d}{dt}(f_{1_x}) P_{0/0} \frac{d}{dt}(f_{1_x}^T) \tag{3-14}$$

where $K << 1$, usually $K = 10^{-6}$.

IV

COMPUTATIONAL METHODS

The propagation of the state has been made by numerical integration of the Cowell Equations of motion and the state transition matrix by numerical integration of the variational equations.

To obtain accurate propogation of the state using the least possible computer time, two different integration methods as well as two force models have been used.

These two options are:

1. Numerical integration by a fourth order Runge-Kutta of the equations of motion and variational equations with a gravity field including only J_2 for equations of motion and variational equations.

2. Numerical integration by a 12th order summed Adams-Cowell predictor-pseudo corrector of the equations of motion and using an 8th order summed Adams-Cowell corrector only for variational equations, the gravity field being 4 by 4 for equations of motion and J_2 only for variational equations.

The decision to use one or the other was made by evaluating the number of times that the forces had to be evaluated in each case to perform a given propagation taking into account the different force model used in each case.

It was decided to use option 1 only if the number of force evaluations was less than or equal to forty for the propagation to the next data point.

It is possible to have a good estimate of this number by assuming the step size used in option (1) satisfies:

$$h = Q R^2/\mu, \quad Q = \begin{cases} 0.05 & e < 0.2 \\ 0.01 & e \geq 0.2 \end{cases}$$

V

CASES STUDIED

Three different satellites have been studied in this paper. Two of them have very high eccentricity (RAE-B and IMP-J, transfer orbit), and the third is a near circular, almost polar orbit (ERTS-1).

1) The initial conditions for each of these satellites follow.

a) RAE-B

Epoch: June 10, 1973 - 15 hr. 22 min. 19.9461 sec.

Initial state:

a_0	=	198835.0	Km	X_0	=	-19587.57 Km
e_0	=	.9669928		Y_0	=	- 2927.08 Km
i_0	=	29.11926	deg.	Z_0	=	- 8341.75 Km
Ω_0	=	319.3744	deg.	$\dot{X}_0$	=	- 3.584823 Km/sec.
ω_0	=	118.5193	deg.	$\dot{Y}_0$	=	- 3.735018 Km/sec.
M_0	=	1.321811	deg.	$\dot{Z}_0$	=	- 2.879267 Km/sec.

Coordinate system: Mean equator of 1950

Four different initial covariance matrices have been used. P_{0_3} and P_{0_4} are chosen arbitrarily to be diagonal. P_{0_1} and P_{0_2} are computed by means of a simulation starting with P_{0_3} and P_{0_4}. The procedure is to start with the epoch June 10, 1973, 25 hr 22 min 19.9461 sec and integrate the state backwards to June 10, 1973, 14 hr 28 min 47.966 sec. At this time initialize the filter with P_{0_3} and P_{0_4}. Propagate these to the original epoch. These propagated values are then used for P_{0_1} and P_{0_2}. This procedure helps to eliminate the transient response of the filter.

b) IMP-J

Epoch: September 26, 1973 - 2 hr. 38 min. 15 sec.

Initial state:

a_0	=	124510.0	Km	X_0	=	5649.6 Km
e_0	=	.94719		Y_0	=	2453.8 Km
i_0	=	.2867085	deg.	Z_0	=	2434.5 Km
Ω_0	=	249.7624	deg.	$\dot{X}_0$	=	- 2.07466 Km/sec.
ω_0	=	120.1121	deg.	$\dot{Y}_0$	=	10.1934 Km/sec.
M_0	=	.08634	deg.	$\dot{Z}_0$	=	2.9925 Km/sec.

Coordinate system: Mean equator of 1950

The initial covariance matrix (Table 2) was calculated by the Monte Carlo method.

c) ERTS-1

Epoch: August 9, 1972 - 15 hr. 15 min. 0 sec.

Initial state:

a_0	=	7283.213	Km	X_0	=	1906.134	Km
e_0	=	.001863498		Y_0	=	-4009.233	Km
i_0	=	98.99210	deg.	Z_0	=	-5789.823	Km
Ω_0	=	283.5776	deg.	$\dot{X}_0$	=	.7200720	Km/sec.
ω_0	=	148.0186	deg.	$\dot{Y}_0$	=	- 5.932595	Km/sec.
M_0	=	158.4419	deg.	$\dot{Z}_0$	=	4.338789	Km/sec.

Coordinate system: Mean equator of 1950

Two different covariance matrices (P_{0_1} , P_{0_2}) have been used for this case.

P_{0_1} has been calculated in the same way as P_{0_1} and P_{0_2} for RAE-B. The state was projected back to August 9, 1973 - 13 hr. 31 min. 0 sec.
P_{0_2} has the same diagonal as P_{0_1} but the off- diagonal elements are zero.

2) The observations used for each satellite follow.

a) RAE-B

Observation span:

Start time: June 10, 1973 - 15 hr. 22 min. 20 sec.
End time : June 11, 1973 - 2 hr. 38 min. 46.254 sec.

Total number of observations: 233
Data types: VHF range (ρ), range rate ($\dot{\rho}$) and minitrack direction cosines (ℓ ,M)

From a statistical point of view these observations are not good and it is difficult to get a D.C. solution from them. Some biases appeared as:

- CARVON range bias of 480 m.

- CARVON range rate bias of 1.32 m/sec.
- MADGAR range rate bias of .32 m/sec.

The distribution of these observations is nonuniform.

The measurement standard deviations are:

σ_ρ = 150 m σ_ℓ = 0.0003 radians
$\sigma_{\dot\rho}$ = 20 cm/sec. σ_M = 0.0003 radians

b) IMP-J

Observation span:
Start time: Sep. 26, 1973 - 3 hr. 2 min. 21.052 sec.
End time : Sep. 26, 1973 - 11 hr. 35 min. 37.254 sec.

Total number of observations: 387
Data type: VHF and Minitrack

These observations are similar in quality to the previous ones. Biases appeared smaller and were not taken into account.

Two sets of measurement standard deviations were assumed:

1. New:

σ_ρ = 100 m σ_ℓ = 0.0001 radians
$\sigma_{\dot\rho}$ = 20 cm/sec. σ_M = 0.0063 radians

2. Standard:

σ_ρ = 500m σ_ℓ = 0.0003 radians
$\sigma_{\dot\rho}$ = 30 cm/sec. σ_M = 0.0003 radians

c) ERTS-1

Observation span:
Start time: Aug. 9, 1973 - 15 hr. 15 min. 0 sec.
End time : Aug. 9, 1973 - 23 hr. 26 min. 0 sec.

Total number of observations: 863
Data type: USB range and angles

These observations are the best of the three cases. No biases appeared, but the Y angle measurement did not improve the solution.

Two sets of measurement standard deviations were assumed:

1. New:

σ_ρ = 10 m

$\sigma_{x_{30}}$ = 100 sec. of arc.
$\sigma_{y_{30}}$ = 100 sec. of arc.

2. Standard:

σ_ρ = 20 m

$\sigma_{x_{30}}$ = 200 sec. of arc.
$\sigma_{y_{30}}$ = 200 sec. of arc.

In all the cases measurements were corrected by

- Refraction
- Transponder delay
- Light time

The observations were edited by:

- Elevation angle
- Amount of the refraction correction
- k_σ criterion, i.e., the residual must satisfy

$$y_k - h(x_{k/k-1}) \leq k_\sigma (h_x P h_x^T + \sigma_k)^{1/2}$$

VI

RESULTS

The filter errors plotted in Figures 1 through 25 are the result of comparing the filter estimate with the DC (iterated weighted least squares) solution. These DC solutions have been chosen as "true solutions" for lack of better information. The observation spans used for these solutions were longer than those used in the filter runs.

The ERTS-1 DC solution is more reliable than those for RAE-B and IMP-J, but the wider scale errors for these two satellites make the results equally reliable. In Figures 1 through 20 are plotted differences between the filter estimates and the DC solution

a. Along track:

$$(R_F - R_{DC}) \cdot V_{DC} \; | V_{DC} |^{-1}$$

b. Cross track:

$$| \; | R_F - R_{DC}| - (R_F - R_{DC}) \cdot V_{DC} \; | V_{DC} |^{-1} \; |$$

c. Velocity

$$| V_F - V_{DC} |$$

In Figures 21 through 25 are plotted normalized position and velocity error, that is:

a. Normalized position errors:

$$| R_F - R_{DC} | \cdot (P_{11} + P_{22} + P_{33})^{-1/2}$$

b. Normalized velocity errors:

$$| V_F - V_{DC} | \; (P_{44} + P_{55} + P_{66})^{-1/2}$$

Figures 1 through 10, and 21 through 25 refer to ERTS-1; Figures 11 through 15 to RAE-B, and Figures 16 through 20 to IMP-J.

Figures 1, 2 and 3 compare the errors for the three different filters tested in this study, for ERTS-1. The improvement of MEKF appears slight, but both

of them show great differences from MJF. From observation 243 to 244 there is a time difference of 5 hr. 15 min.; from 516 to 517, 1 hr. 26 min., and from 736 to 737, 39 min. These three gaps may be seen clearly in those figures as discontinuities. The three filters are sensitive to them but this sensitivity is much greater for MJF. This could be expected since the approximation made in MJF is good only for short spans of time. For these relatively large gaps the covariance matrix of the state grows too much (the factor is $\sim t^3$ for some terms) making the corrections too large.

Figures 1 and 2 differ in the values assumed for the standard deviations of the observations, σ_ρ = 10 m, $\sigma_{x_{30}} = \sigma_{y_{30}}$ = 100 sec. of arc for Figure 1, and σ_ρ = 20 m, $\sigma_{x_{30}} = \sigma_{y_{30}}$ = 200 sec. of arc for Figure 2 (and 2). K is 3 for these figures and 100 for Figure 3. The sensitivity due to these is not easily explainable unless the characteristics of the observations are taken into account. In this case the Y-angle measurement is very poor while range is the most reliable measurement. By increasing the standard deviations of all of them by the same ratio the filter is opened, this means that more observations are going to be included, but this only favors the inclusion of more Y-angle measurements causing the relative weight of the range to decrease in some stages of the process, thus impairing the solution.

The irregular influence of this factor may also be seen in Figure 7 (EKF) and Figure 8 (MJF).

The precision reached is about 500 m in position and 50 cm/sec. in velocity for EKF and MEKF and about 3 km and 2 m/sec. for MJF, after the first good data (range) of the second station are processed. This happens about the 300th observation. The precision for EKF and MEKF is intermediate between the level of precision used for Range (10 m) and angle (100 sec. of arc $\sim$ 1 km).

The influence of poor angle measurements seems to be stronger in the MJF. $U_{\dot{u}\dot{u}}$ grows too much to adapt to the residuals of this measurement and this is reflected particularly in errors in velocity where there is no direct observability, coupling in the covariance matrix caused by $U_{\dot{u}\dot{u}}$ is more difficult to control in the velocity states.

For RAE-B (Figure 11) differences between the filters seems to be smaller. The noise used for these observations are σ_ρ = 100 m, $\sigma_{\dot{\rho}}$ = 20 cm/sec., $\sigma_\ell = \sigma_M$ = 0.0003. The initial state is quite close to the actual one. Some kind of divergence happens in this case, the position error grows almost steadily from 2 km to about 30 km in the 15 hours of process while the velocity error grows to 750 cm/sec. at the beginning, and ending at about the same level that

it began, 60 cm/sec. However this kind of divergence is different from the result of modeling. In this case it seems to be caused by too few observations.

For IMP-J (Figures 16 and 17) the noises have been the same as those used for RAE-B. In Figure 16, k_σ =100 and Figure 17, k_σ =10. The results shown in Figure 17 are similar to those for RAE-B. The position errors that start at 50 km decrease at the beginning as many good observations are processed, and grow thereafter to about 250 km at the end of 8 hours of data as the observation rate decreases. The velocity errors that started at about 18 m/sec. grow sharply at the beginning then decrease to a level of 16/sec. at the end.

The results with k_σ = 100 (Figure 16) are quite different. After processing 200 observations and tracking the state better than with k_σ = 10 (the position error is now 10 km and the velocity error about 1 m/sec.), the performances of the different filters change completely. The MJF with a covariance matrix which has grown is very sensitive to bad observations and large oscillations begin, thus tracking the state very poorly. The EKF and MEKF continue tracking the state with approximately the same level of error. In this case the EKF shows itself far superior to the other two filters.

The influence of K_σ seems to be different for each case as the characteristics of the observations change. (See Figures 4 (EKF), 5 (MEKF) and 6 (MJF) for ERTS-1; Figure 12 (EKF) for RAE-B, and Figures 18 (EKF) and 19 (MJF) for IMP-J.) When the assumption of white noise on observations is close to reality and enough observations are available as it happens in ERTS-1 data, K_σ =3 is the the best possible value. The inclusion of more observations, or increasing the noise on the observations, or increasing K_σ deteriorates the filter performances. For RAE-B and IMP-J the assumption of white noise is unrealistic, at the same time the observation rate is very low. In this case the EKF and MEKF work much better than MJF and their performances improve from k_σ = 10 to k_σ = 150. For RAE-B the divergence that appeared with k_σ = 10 disappears with k_σ = 150, though the error continues being large (10 km in position and 80 cm/sec. in velocity). In the IMP-J case the improvement is even greater.

The influence of the initial covariance matrix can be seen in Figures 9 (EKF) and 10 (MJF) for ERTS-1 and Figure 13 (EKF) for RAE-B. The EKF and MEKF show greater influence to this parameter than MJF does. The adaptiveness of the MJF causes the initial values to be quickly forgotten. This independence is highly desirable since the initial conditions are not well known. Figure 13 shows how the covariance matrix calculated as described in Chapter V eliminate the transition period.

Although the estimation of parameters other than the state is possible and the filters tested in this study are being implemented to have this capability, only the estimation of biases is available so far. Figure 14 (EKF) and Figure 15 (MJF) for RAE-B and Figure 20 (EKF) for IMP-J show the difference between estimation and no estimation of biases, and it is very simple to deduce that there is not enough information in the observations to estimate these other parameters. The improvement made by the inclusion of estimation of biases is questionable if the data rate is not adequate.

Figures 21 through 25 show how the covariance matrix reflects the actual errors for the different filters in the ERTS-1 case. The errors are normalized with their standard deviations as given by the covariance matrix. Assuming that filter errors are normally distributed the values plotted in these figures should be less than 1 in 66% of the cases. As may be seen in these figures the covariance matrix is too optimistic reflecting the actual filter errors. The difference between actual and expected errors is stronger for EKF, decreases for MEKF and is the least in the MJF as may be seen in Figure 21. Figures 22 and 23 study the influence of k_σ. This factor is more important from this point of view for EKF than for MJF as may be expected. The assumption of larger observation noises makes the covariance matrix reflect a degree of pessimism.

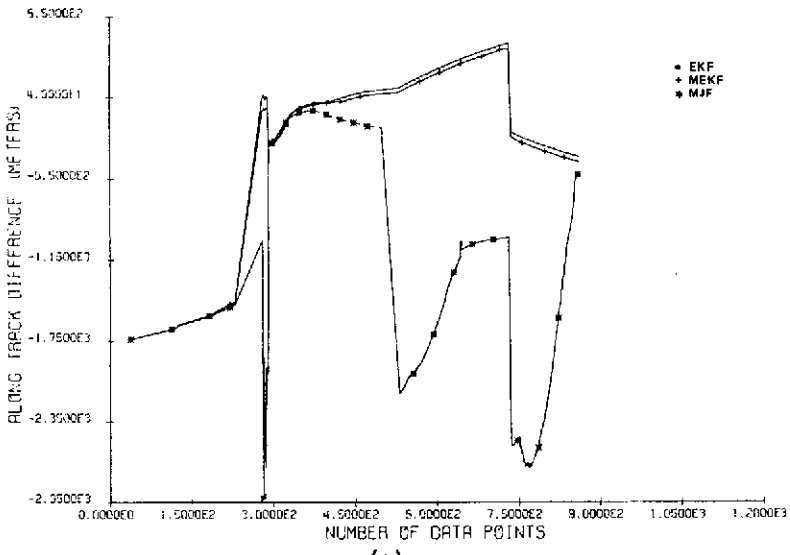

(a)

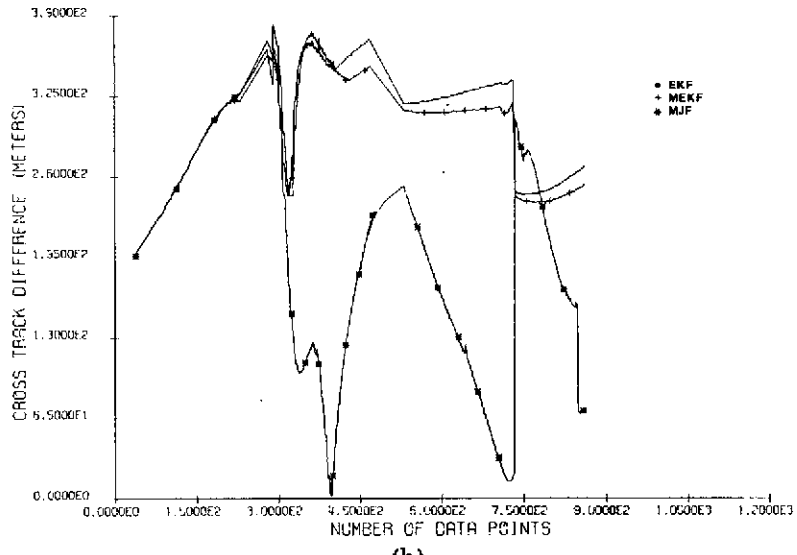

(b)

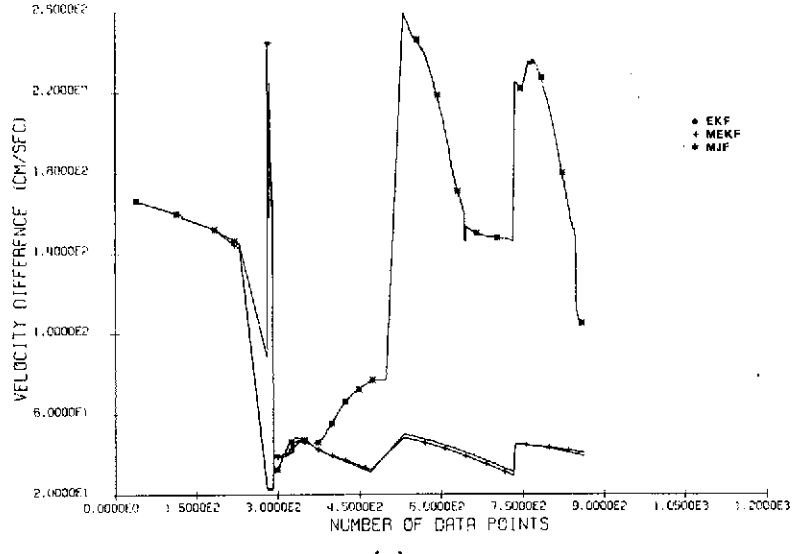

(c)

Figure 1. Comparison of Filter Errors (ERTS-1)

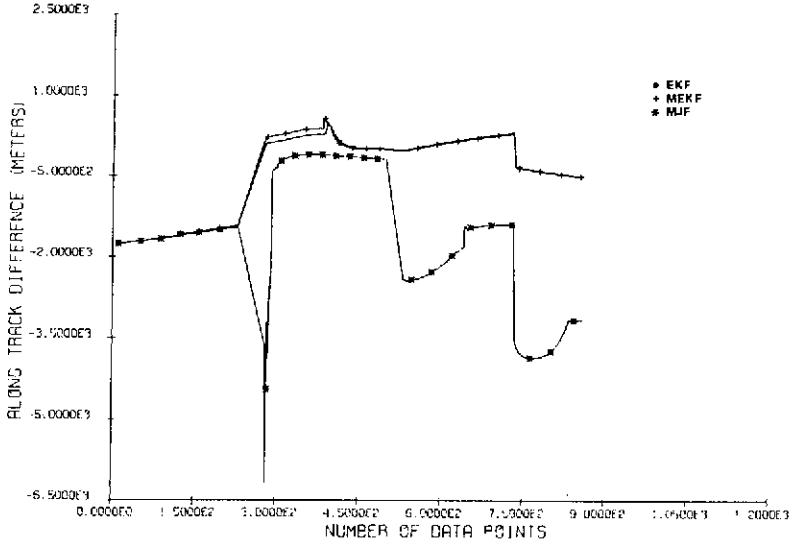

(a)

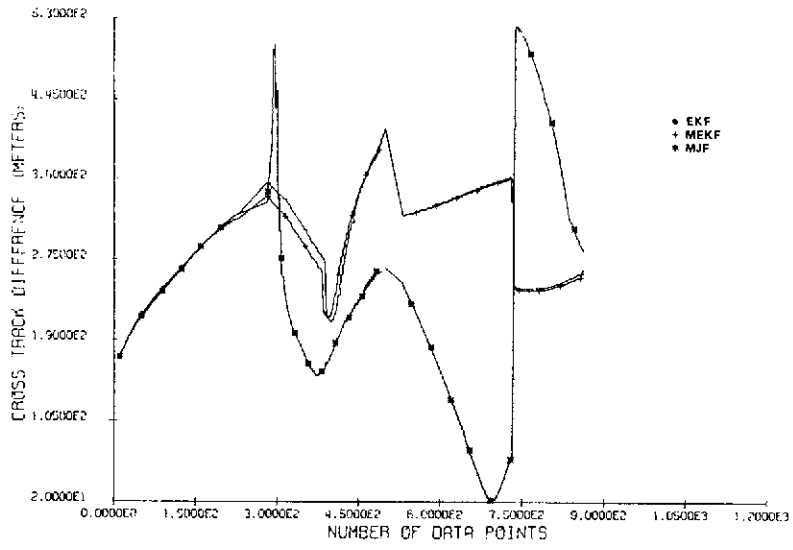

(b)

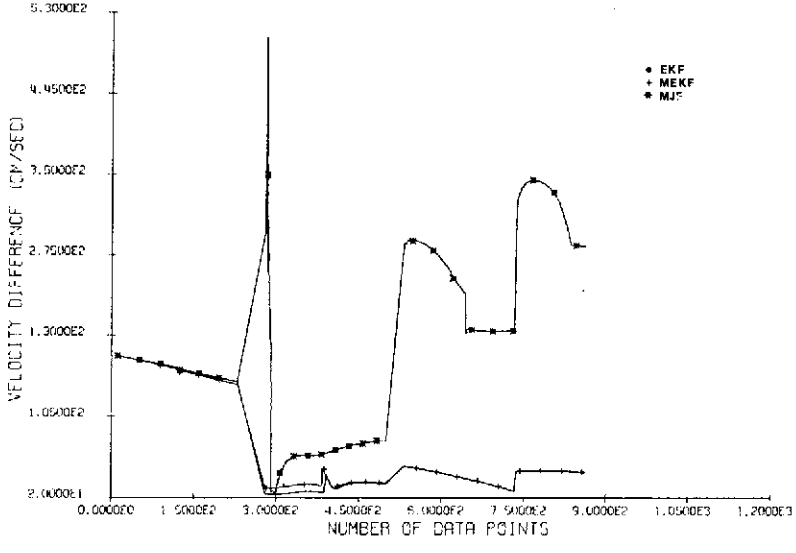

(c)

Figure 2. Comparison of Filter Errors (ERTS-1)

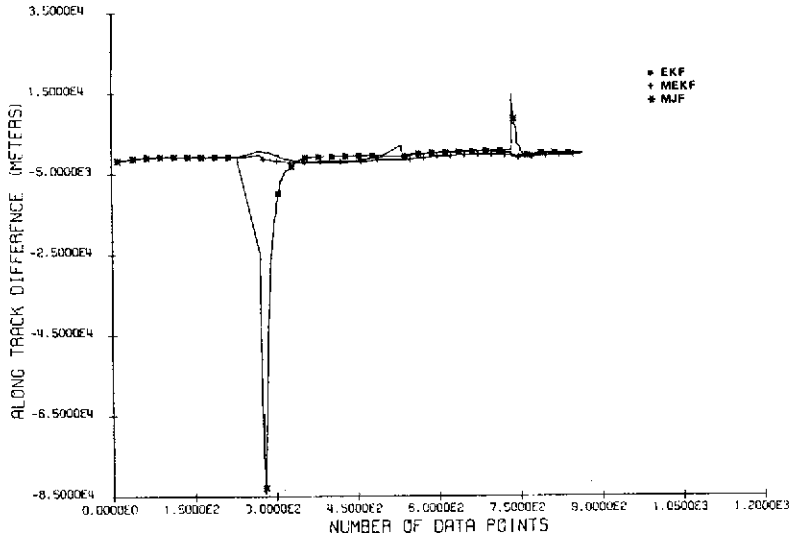

(a)

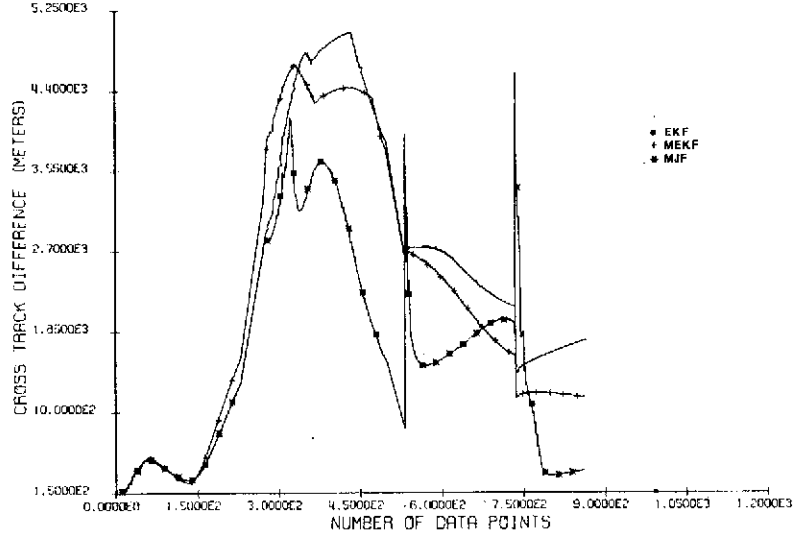

(b)

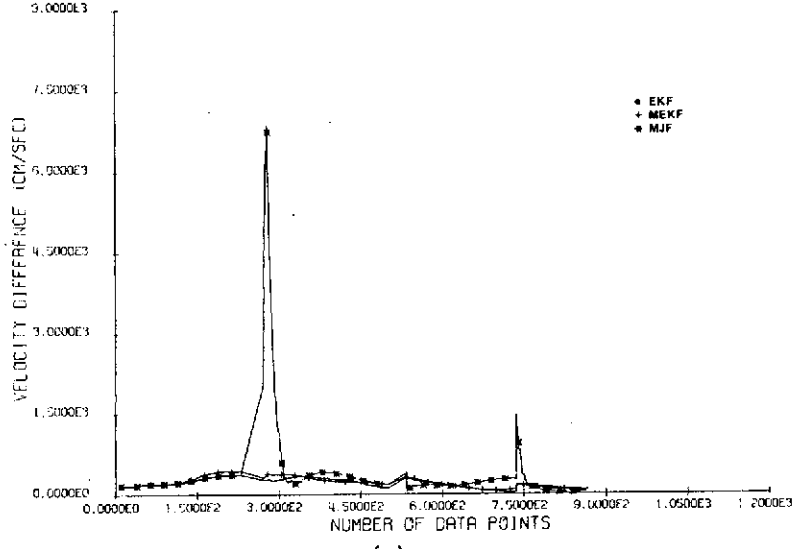

(c)

Figure 3. Comparison of Filter Errors (ERTS-1)

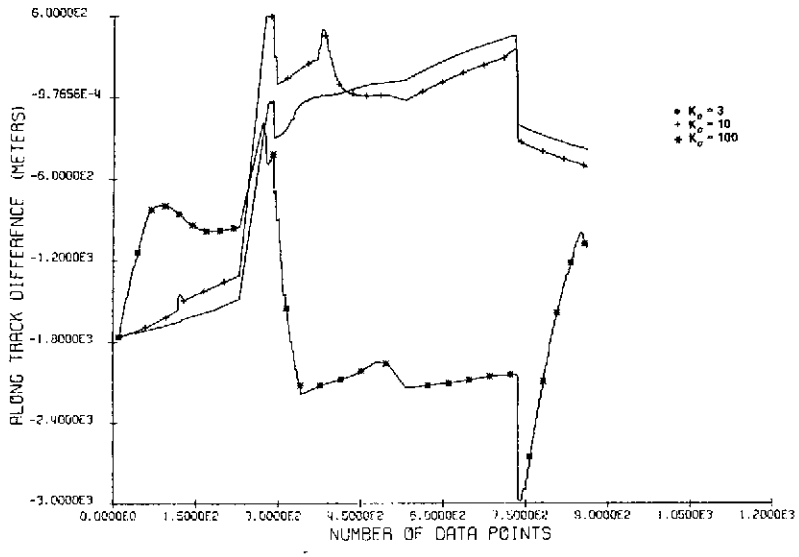

(a)

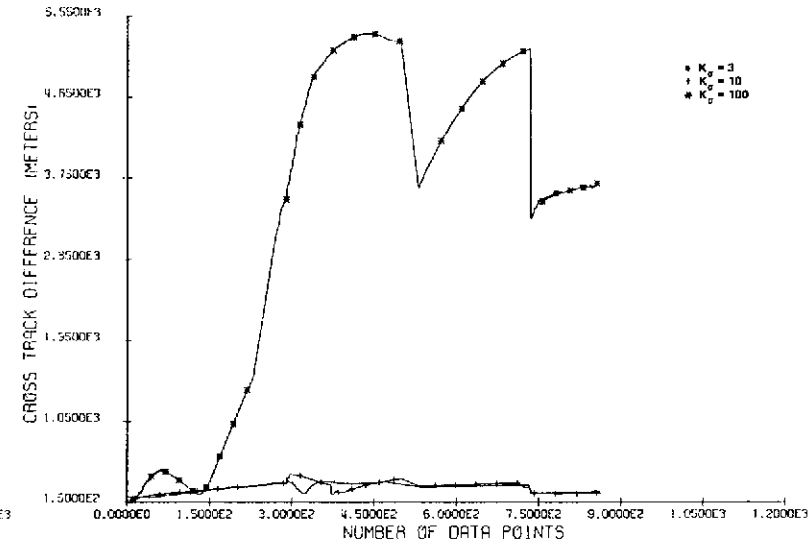

(b)

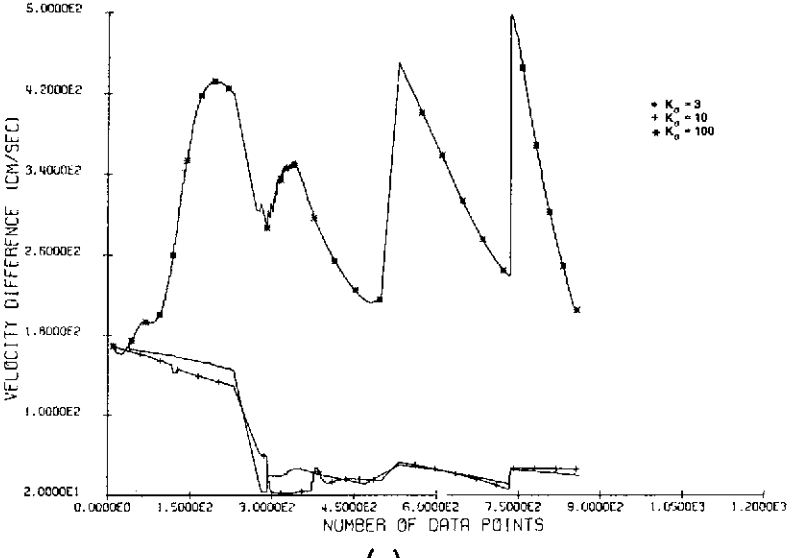

(c)

Figure 4. Comparison of Filter Errors (ERTS-1)

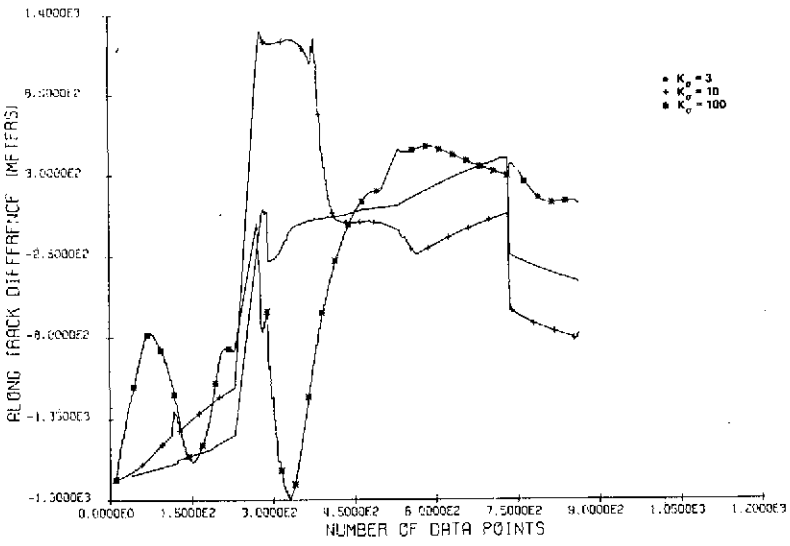

(a)

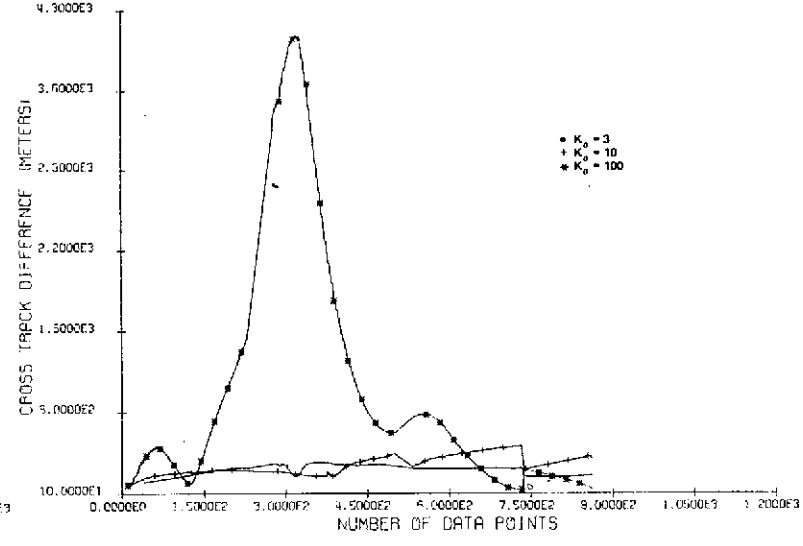

(b)

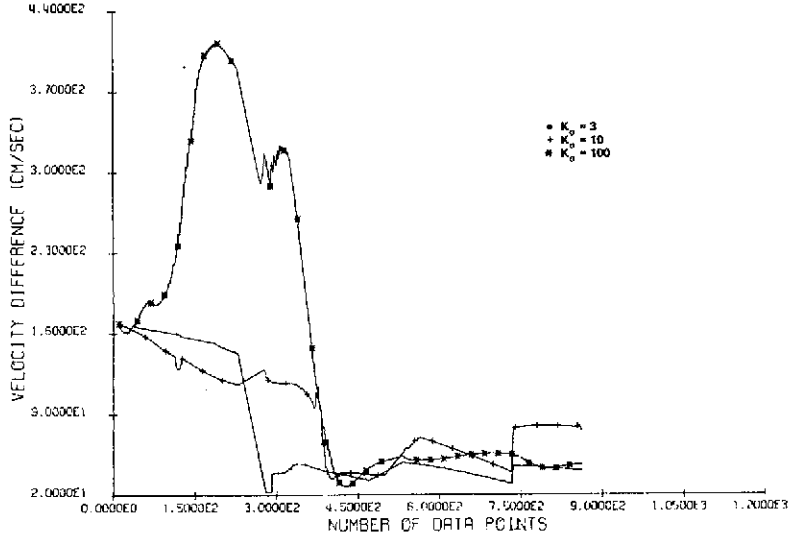

(c)

Figure 5. Comparison of Filter Errors (ERTS-1)

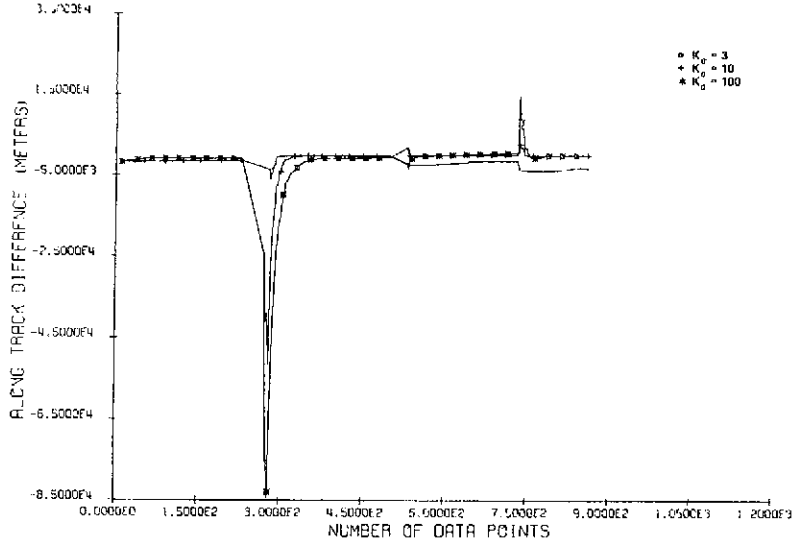

(a)

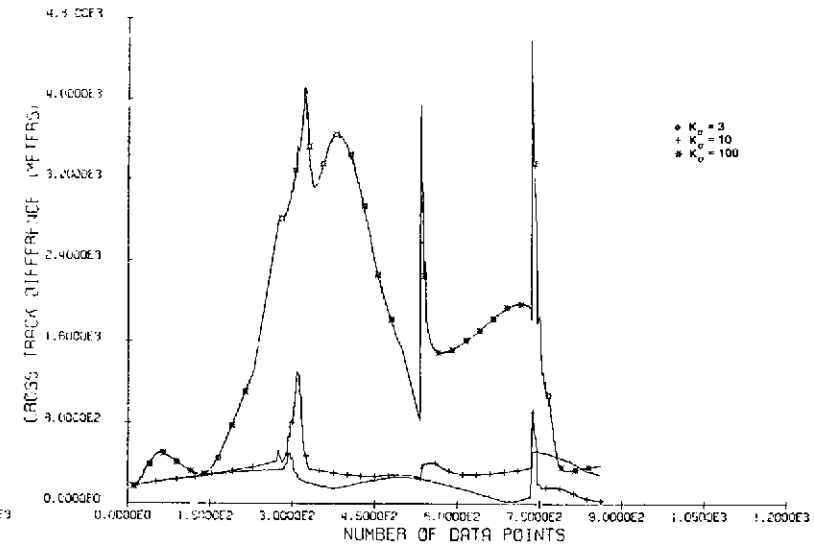

(b)

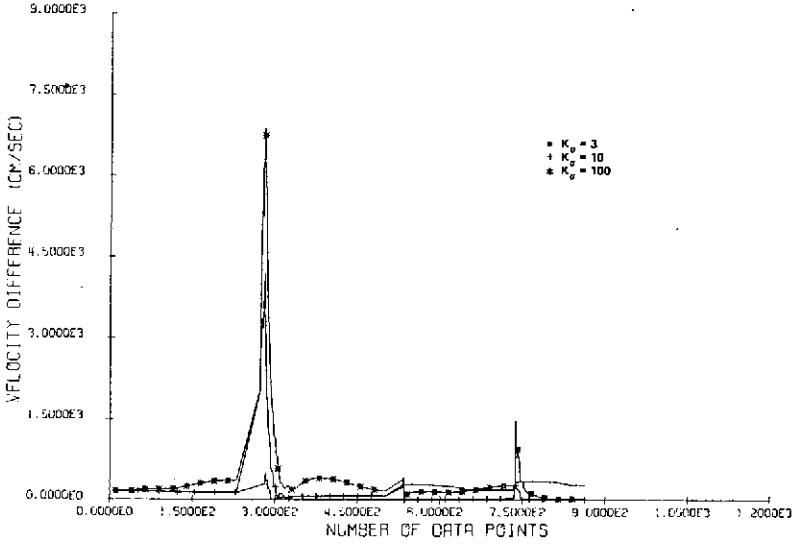

(c)

Figure 6. Comparison of Filter Errors (ERTS-1)

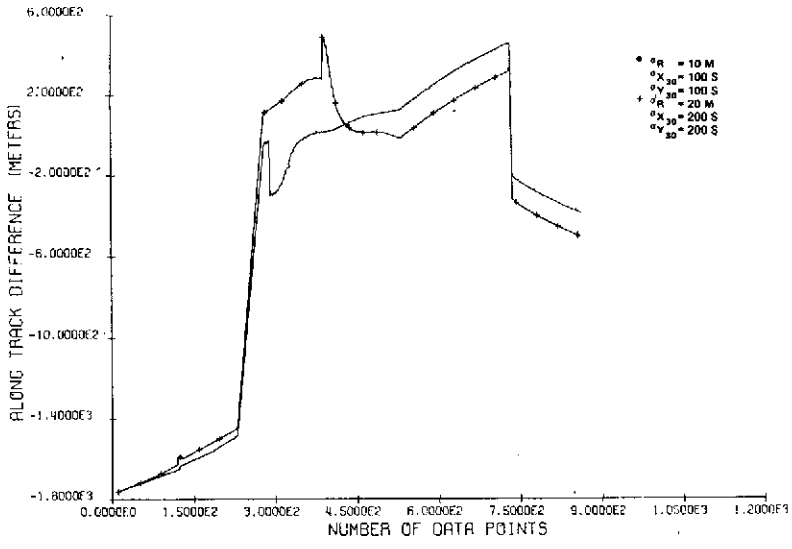

Figure 7. Comparison of Filter Errors (ERTS-1)

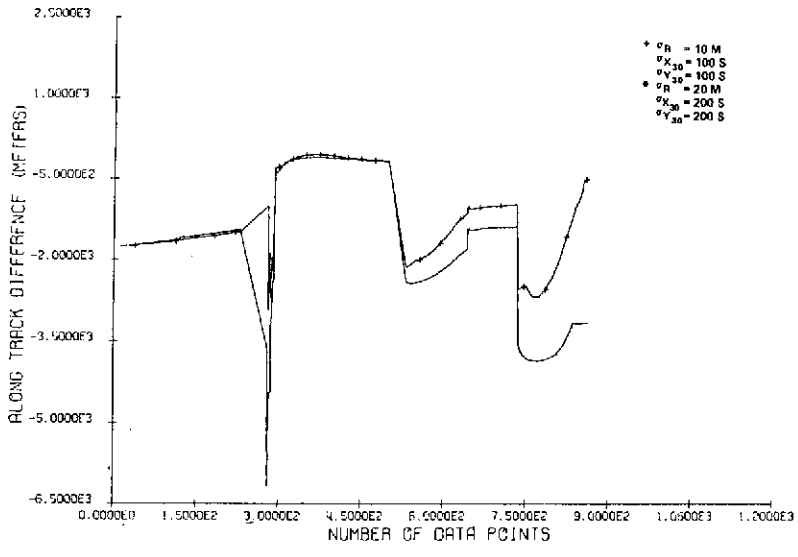

(a)

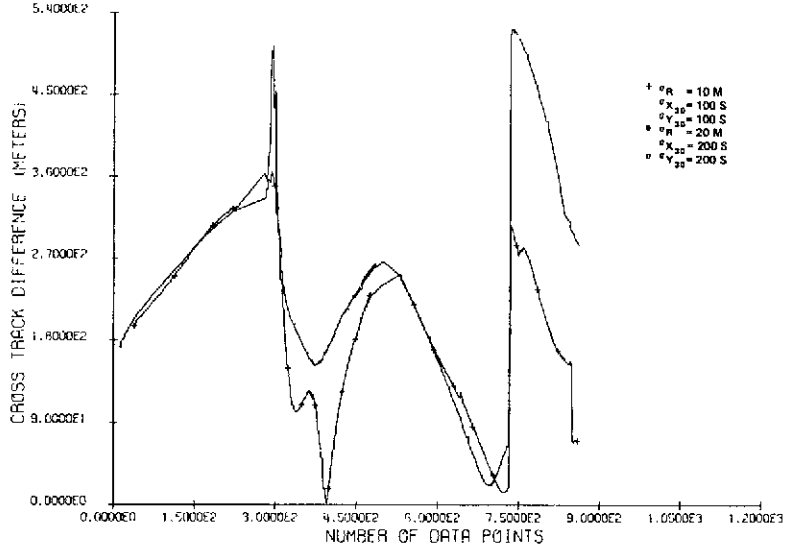

(b)

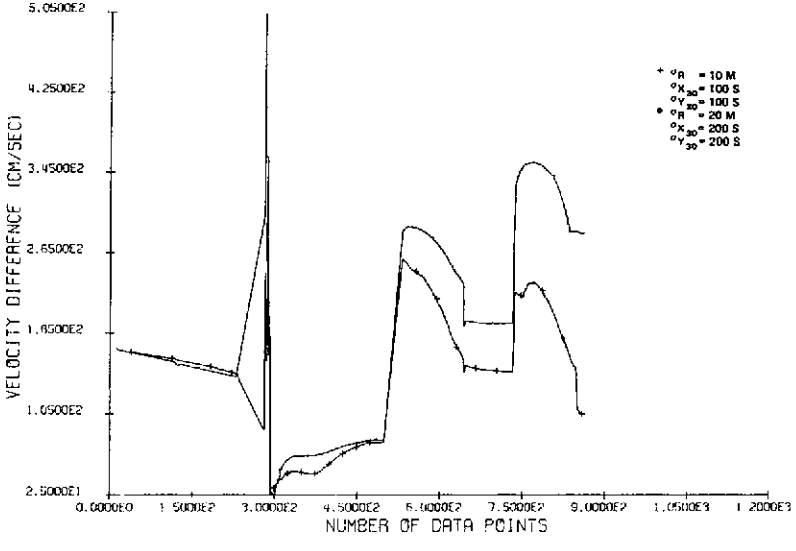

(c)

Figure 8. Comparison of Filter Errors (ERTS-1)

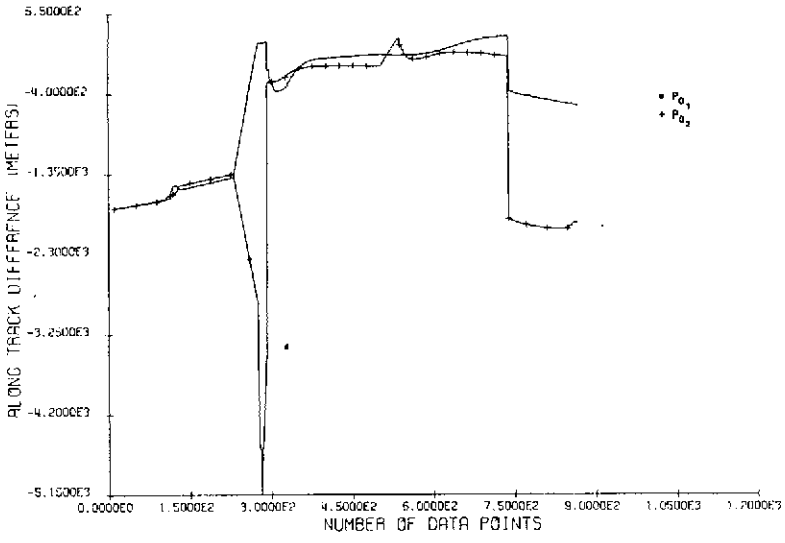

(a)

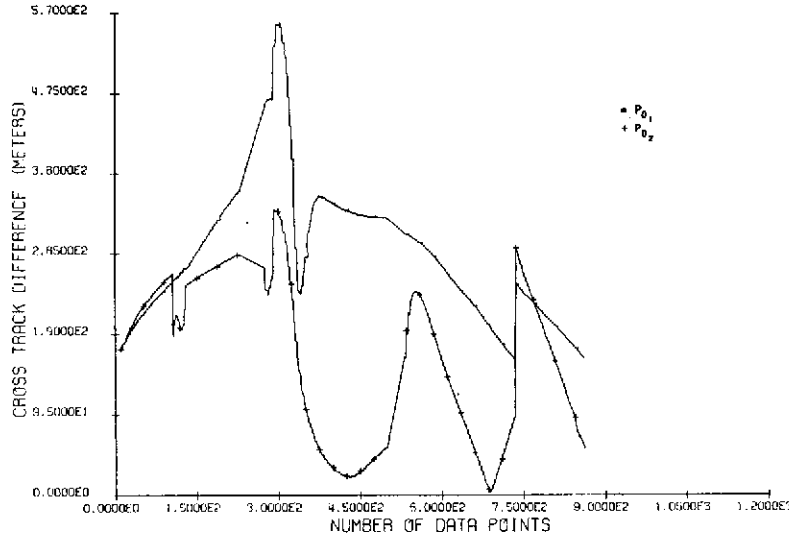

(b)

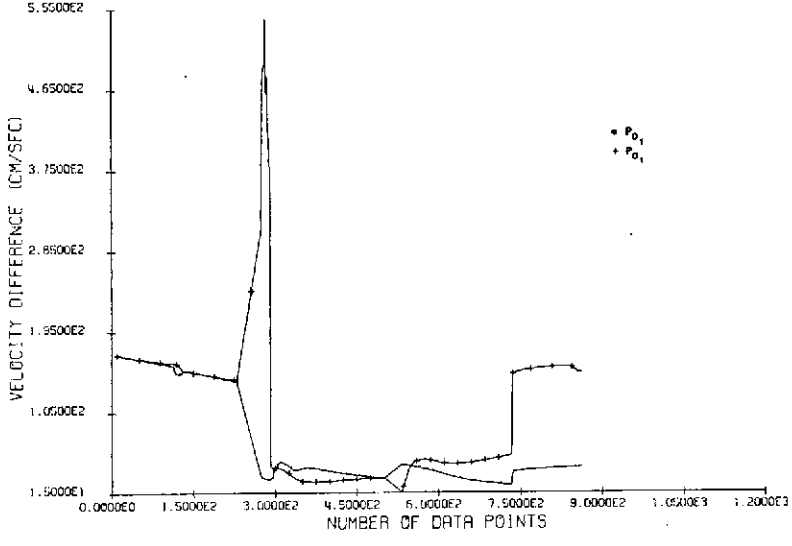

(c)

Figure 9. Comparison of Filter Errors (ERTS-1)

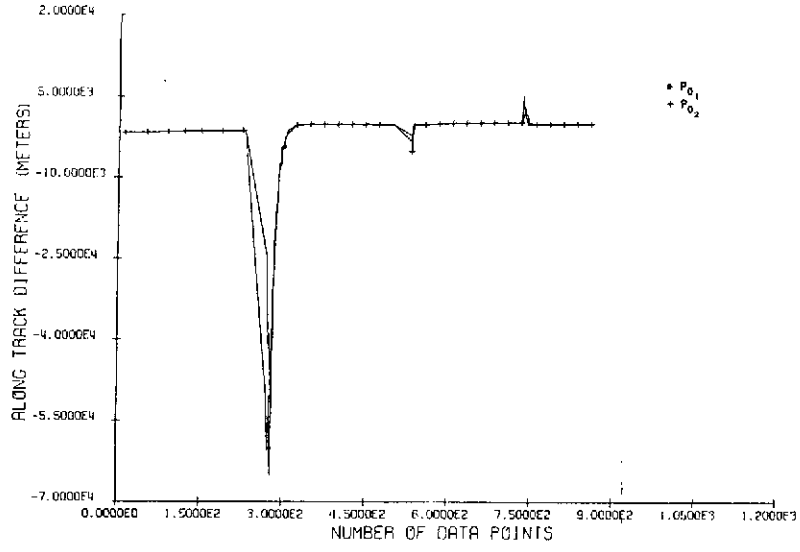

(a)

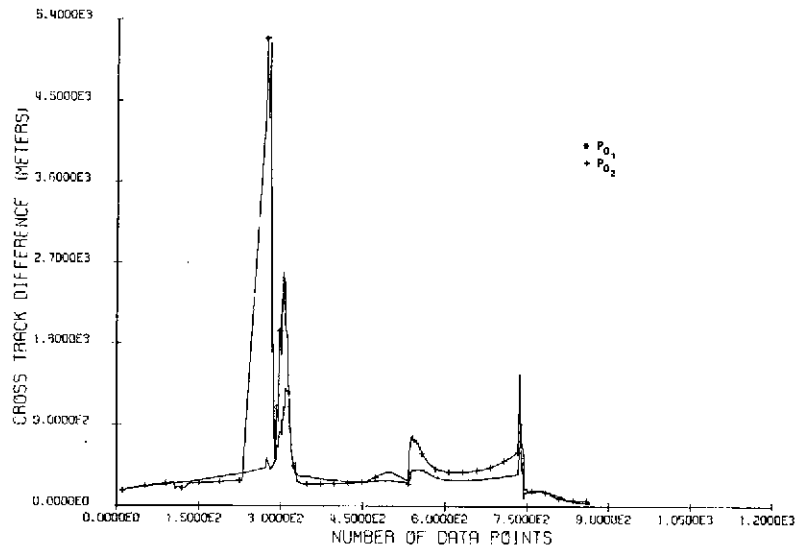

(b)

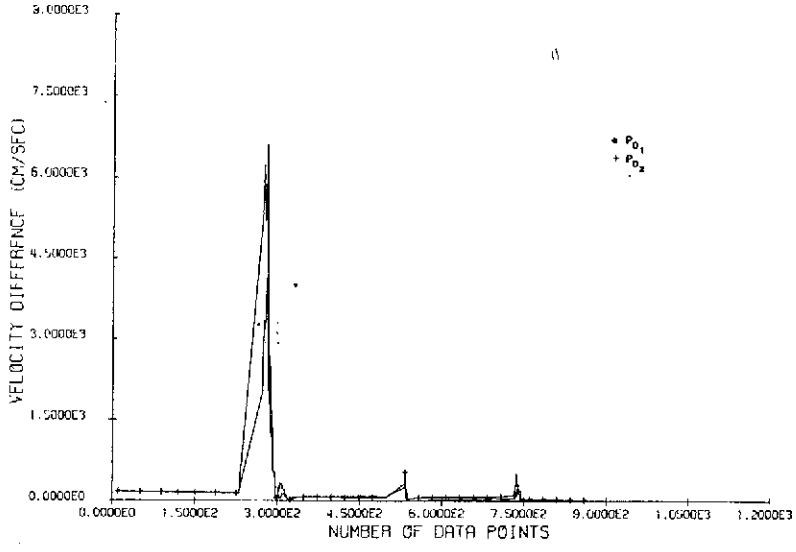

(c)

Figure 10. Comparison of Filter Errors (ERTS-1)

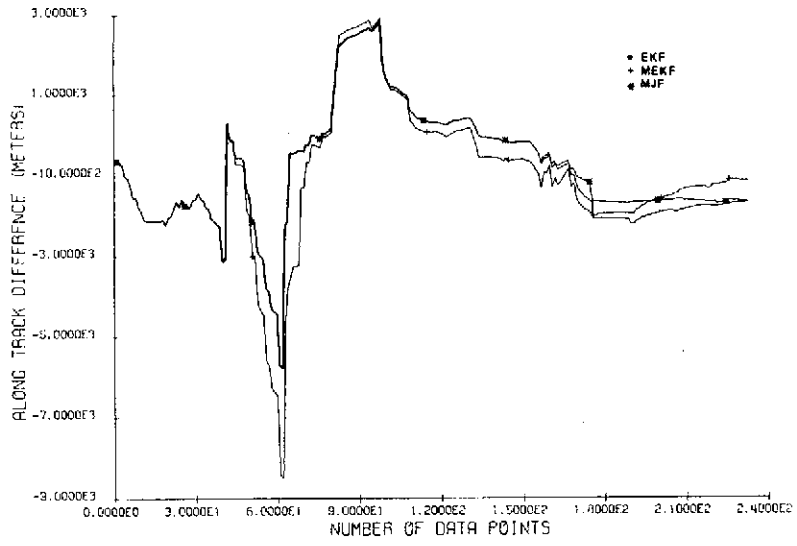

(a)

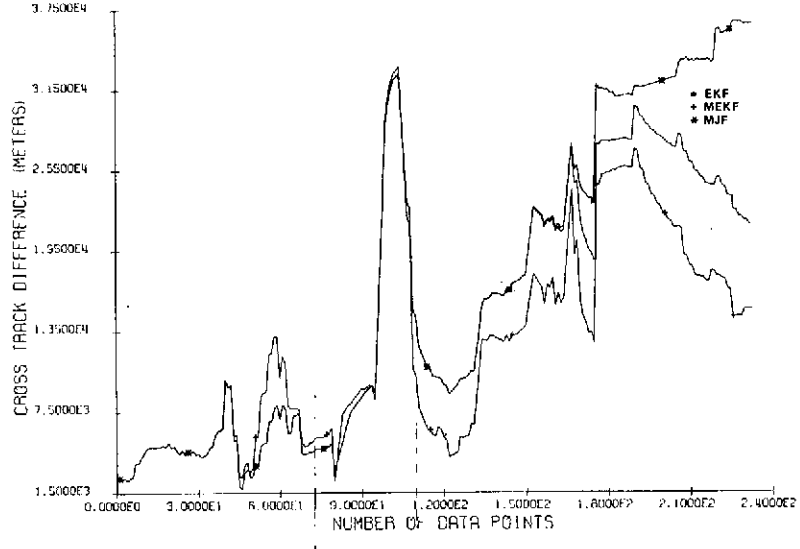

(b)

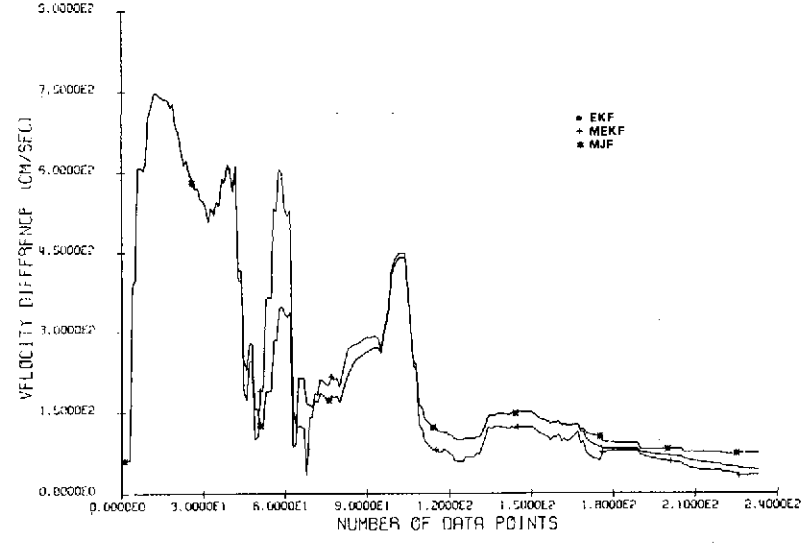

(c)

Figure 11. Comparison of Filter Errors (RAE-B)

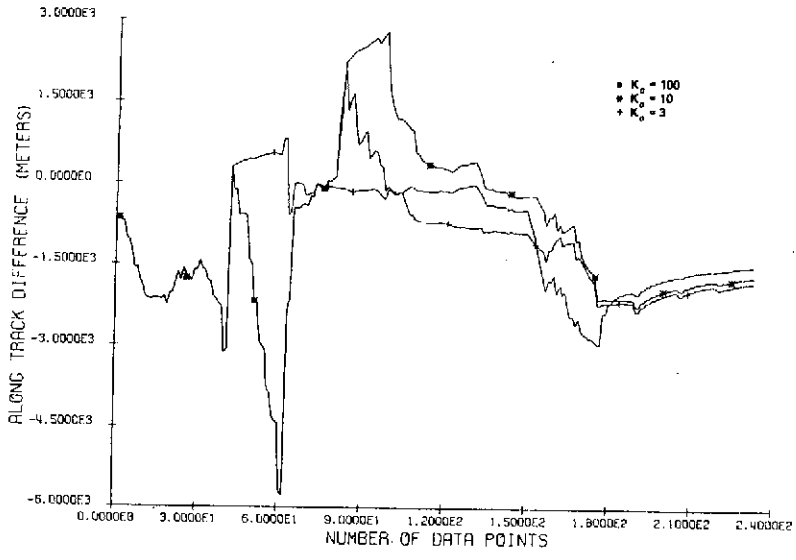

(a)

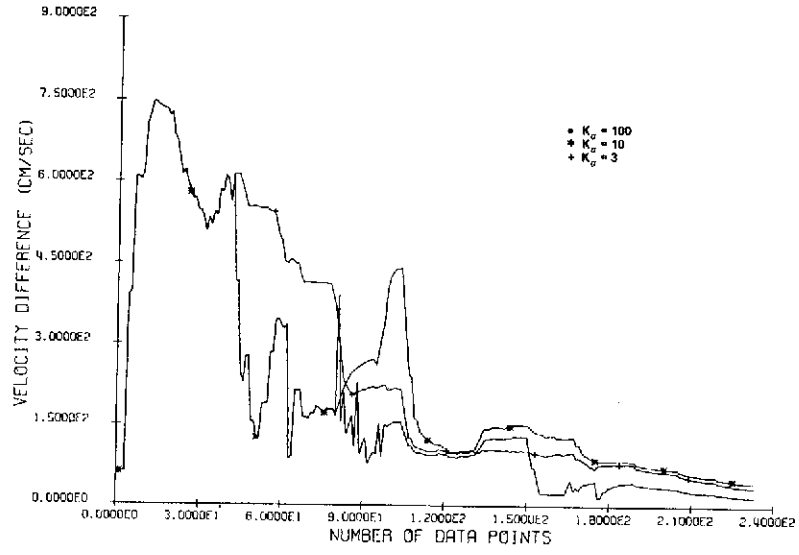

(b)

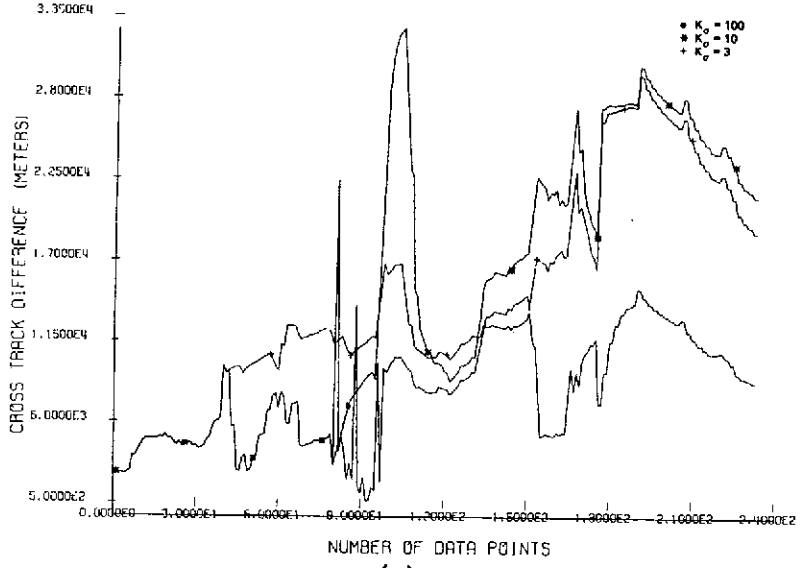

(c)

Figure 12. Comparison of Filter Errors (RAE-B)

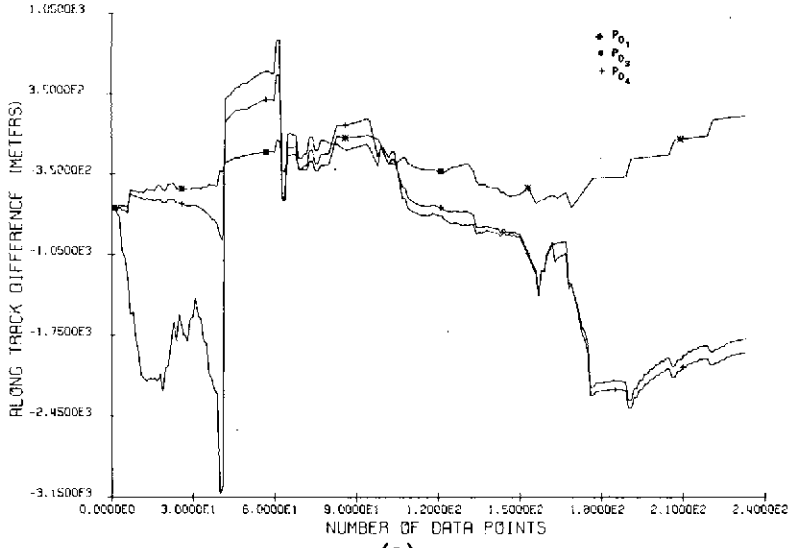

Figure 13. Comparison of Filter Errors (RAE-B)

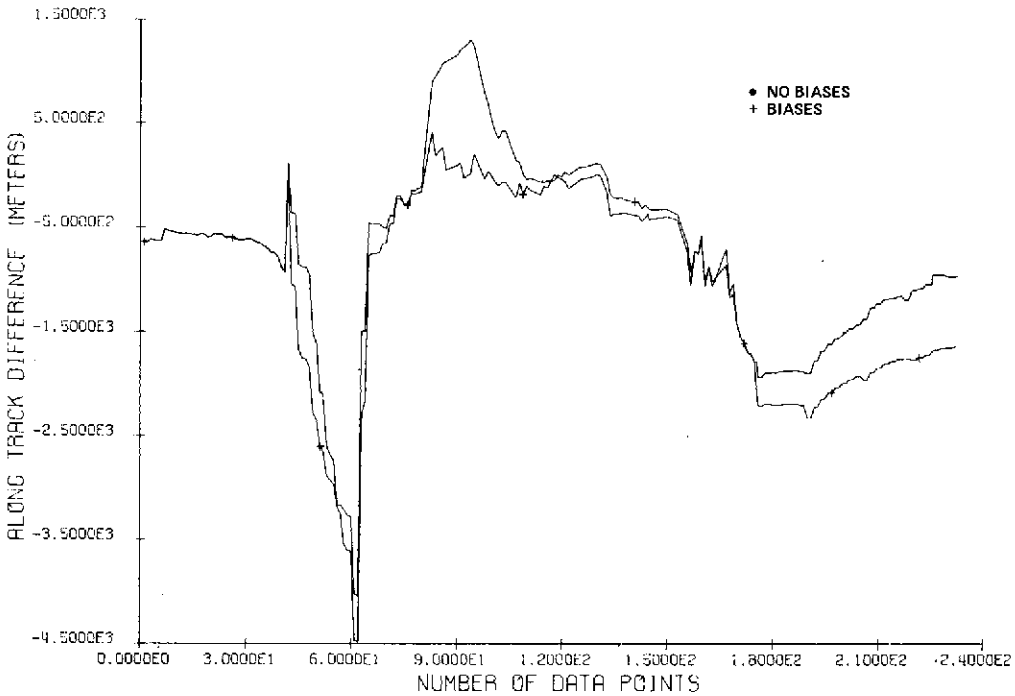

Figure 14. Comparison of Filter Errors (RAE-B)

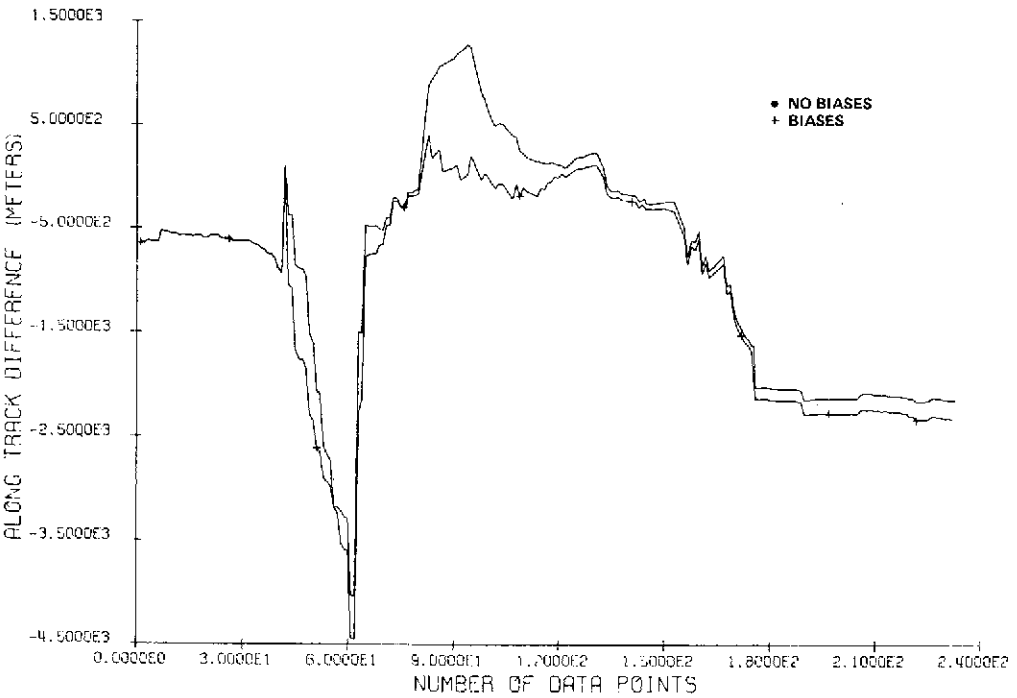

Figure 15. Comparison of Filter Errors (RAE-B)

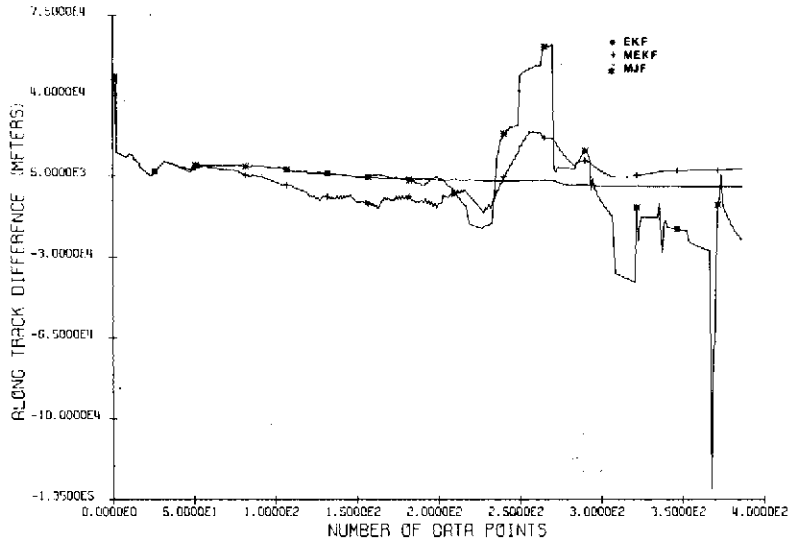

(a)

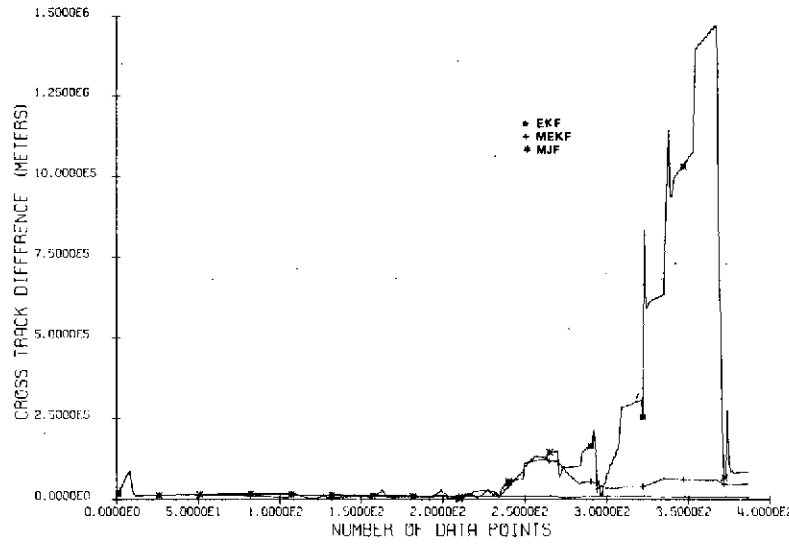

(b)

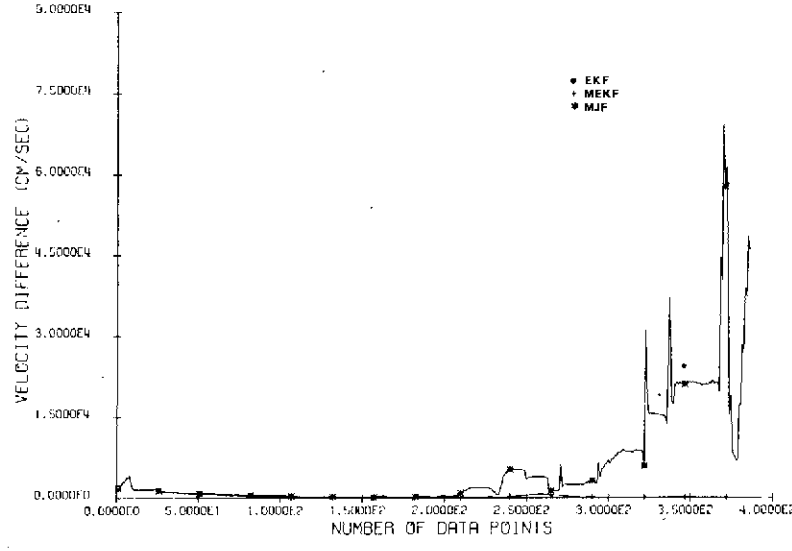

(c)

Figure 16. Comparison of Filter Errors (IMP-J)

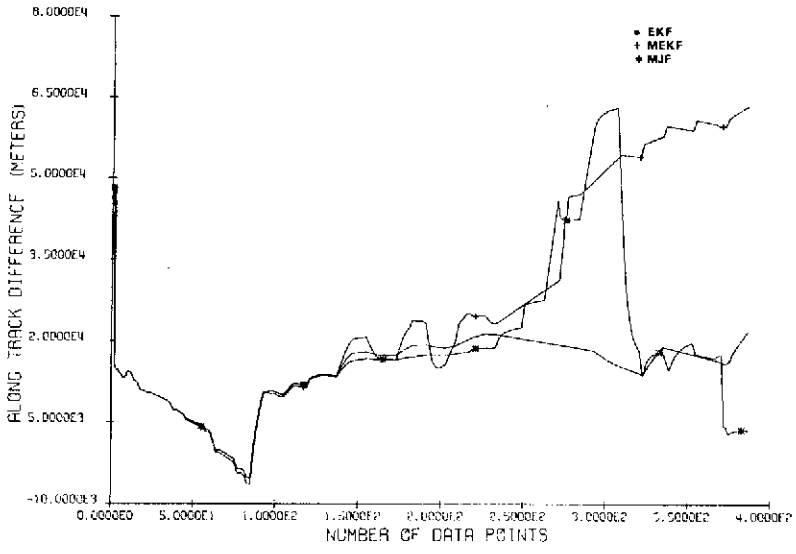

(a)

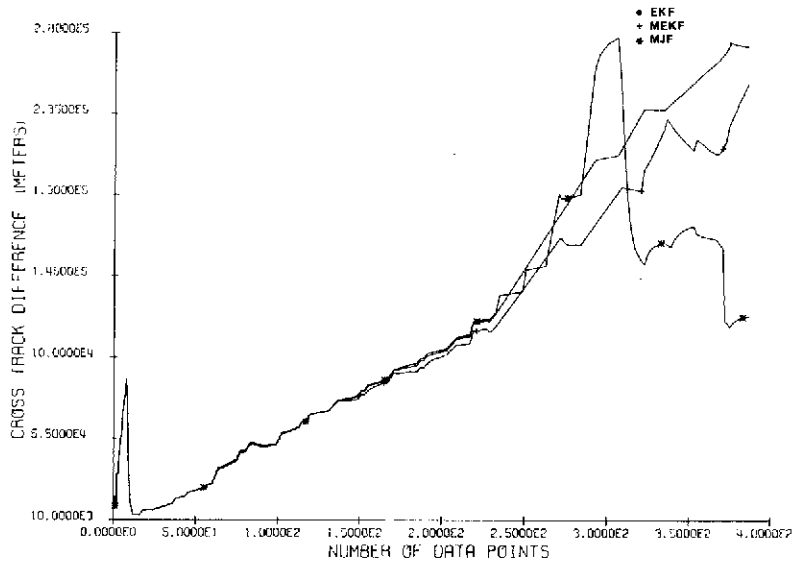

(b)

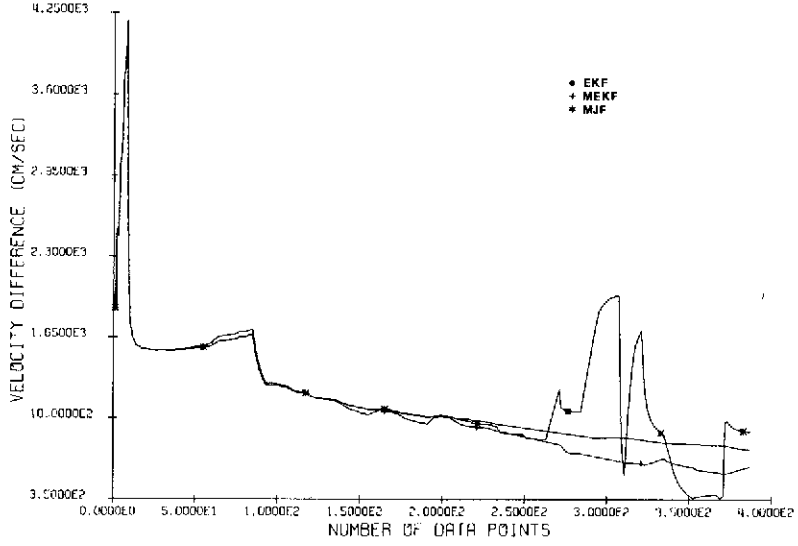

(c)

Figure 17. Comparison of Filter Errors (IMP-J)

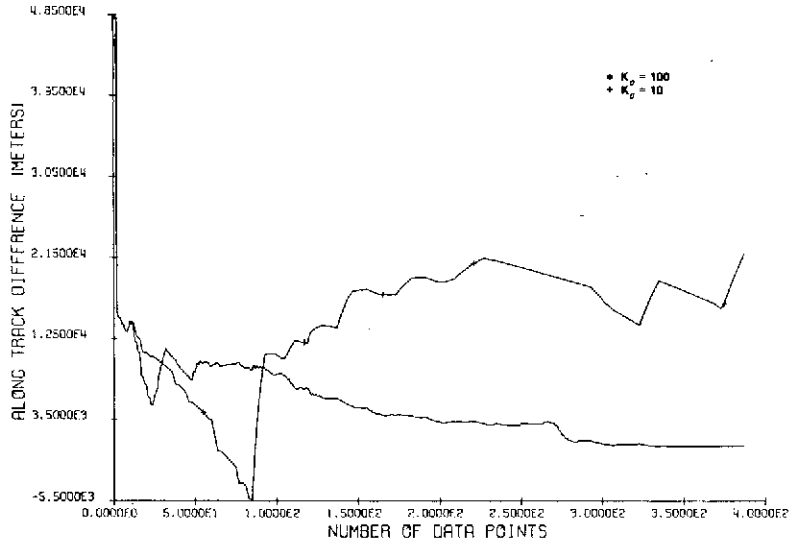

(a)

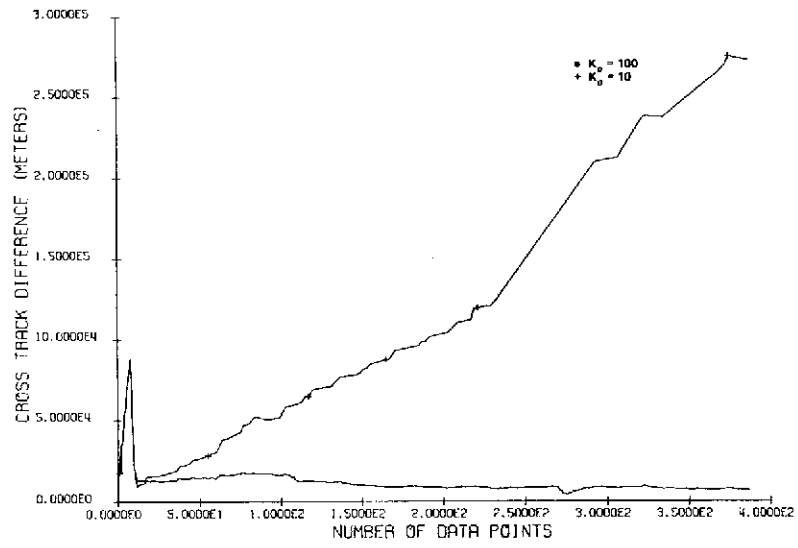

(b)

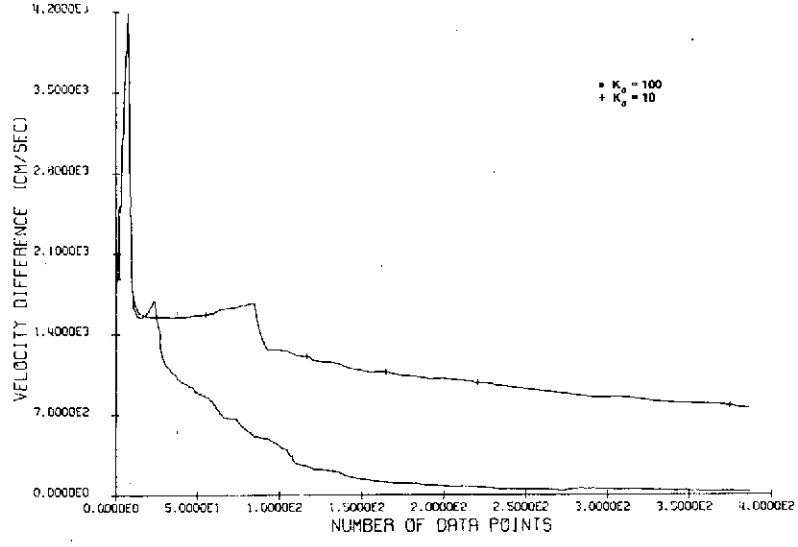

(c)

Figure 18. Comparison of Filter Errors (IMP-J)

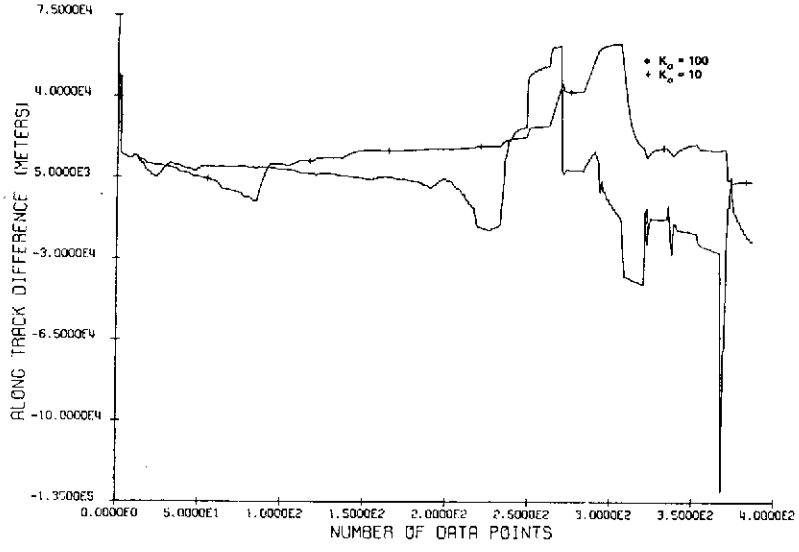

(a)

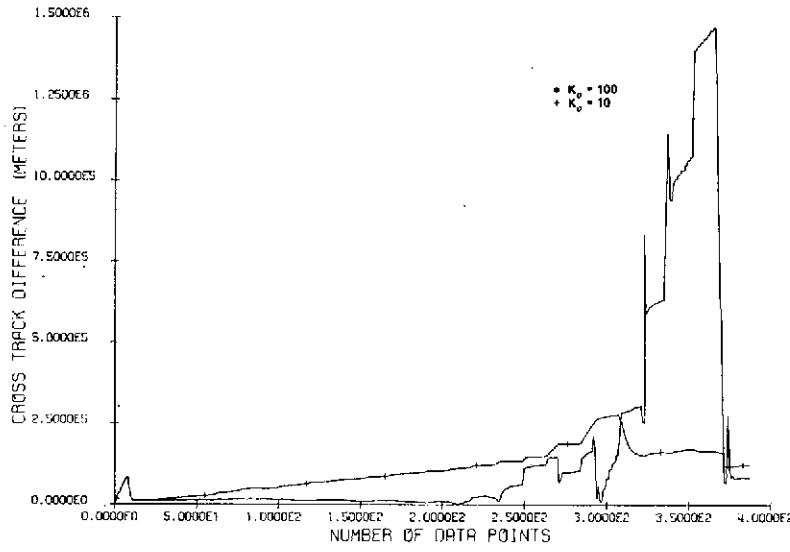

(b)

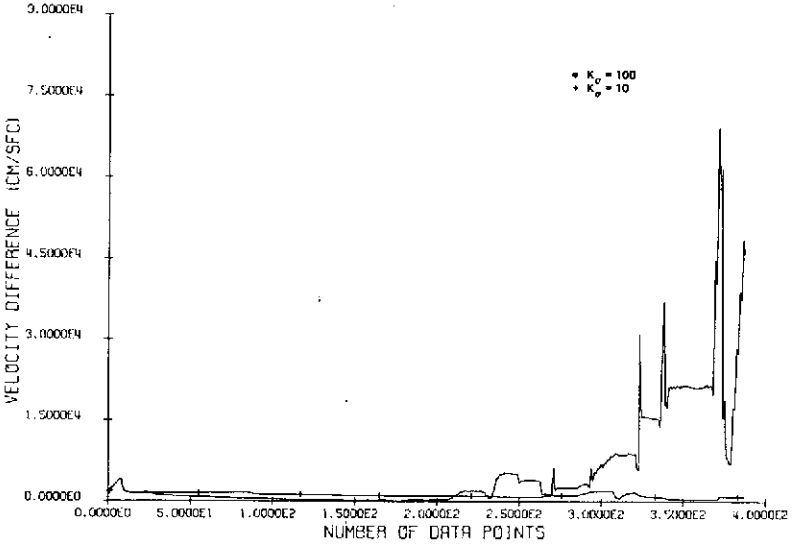

(c)

Figure 19. Comparison of Filter Errors (IMP-J)

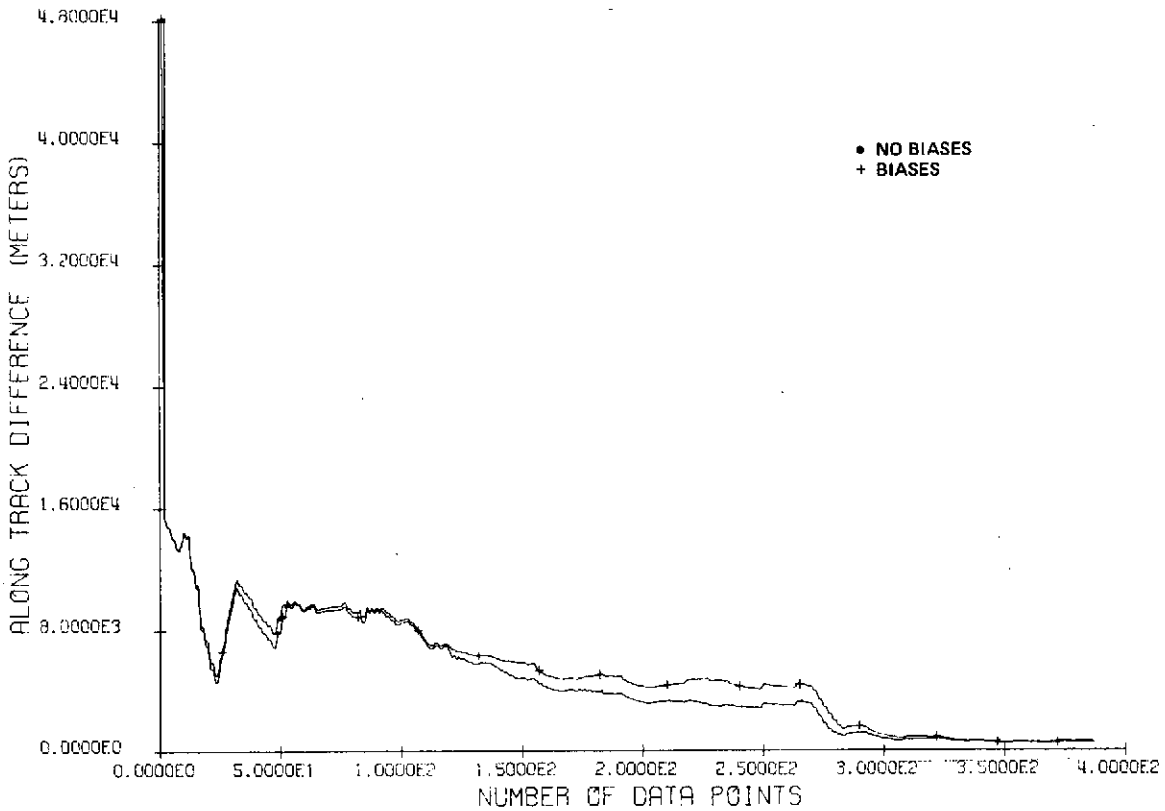

Figure 20. Comparison of Filter Errors (IMP-J)

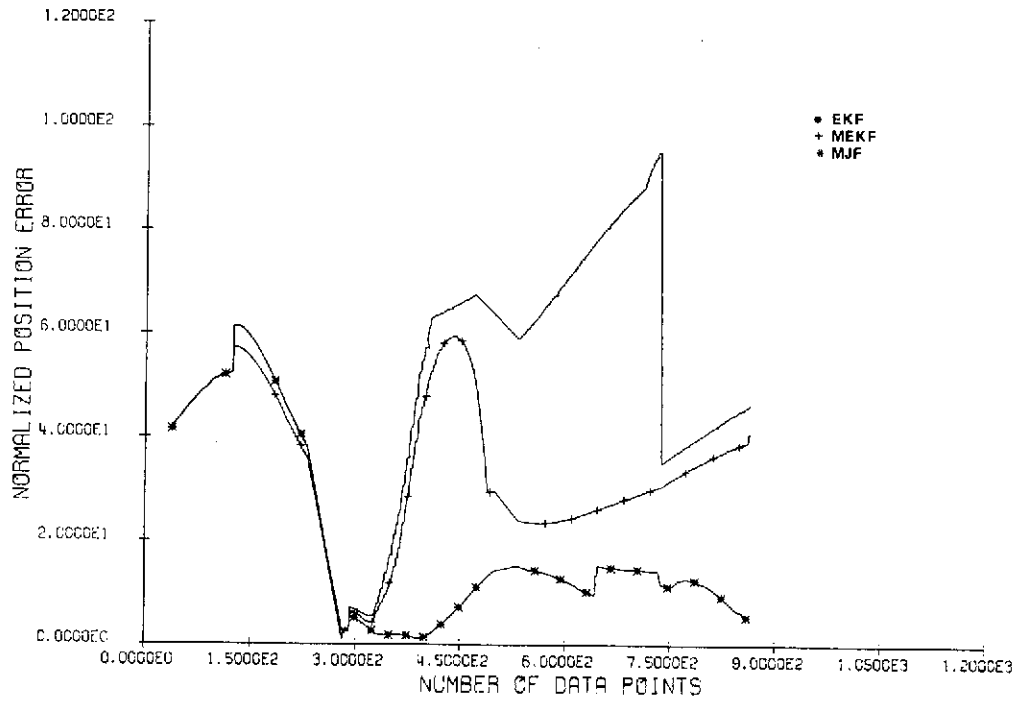

(a)

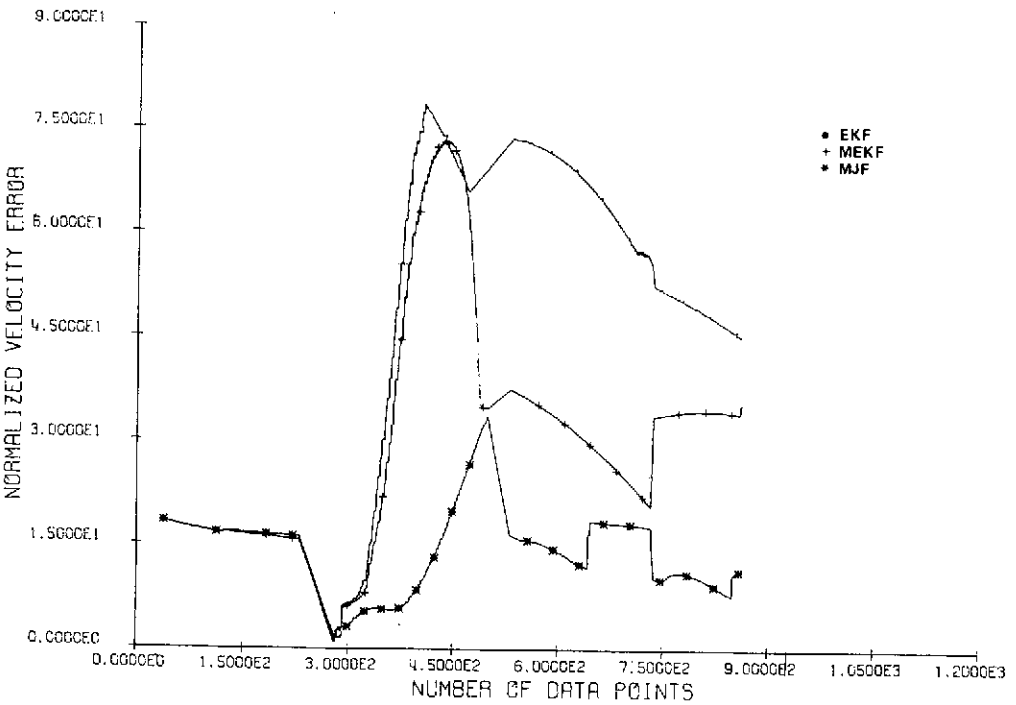

(b)

Figure 21. Comparison of Filter Errors (ERTS-1)

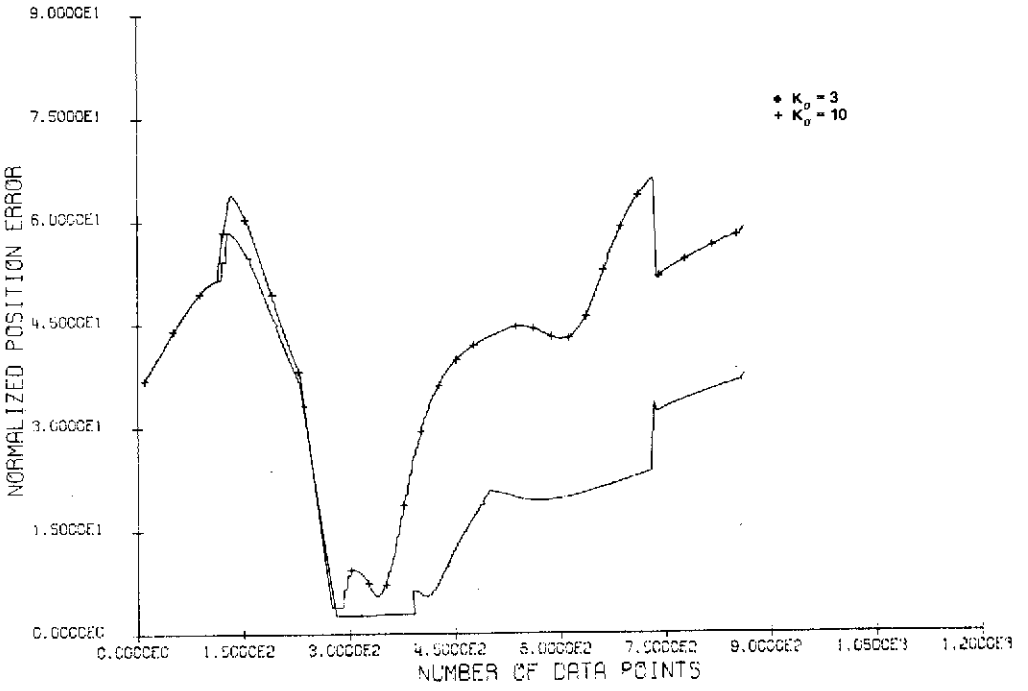

(a)

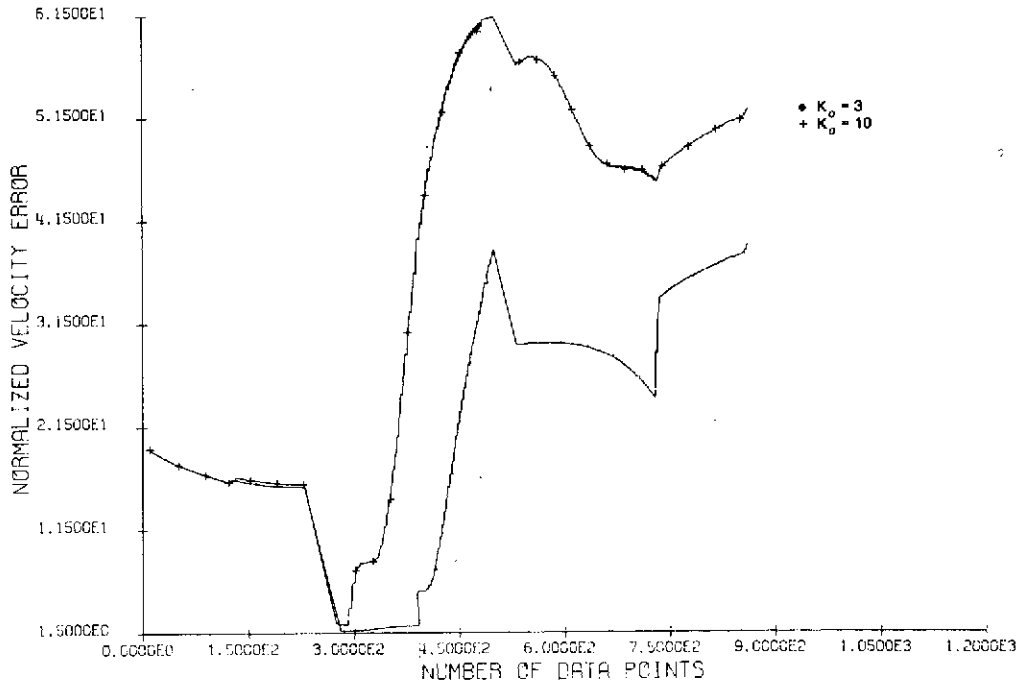

(b)

Figure 22. Comparison of Filter Errors (ERTS-1)

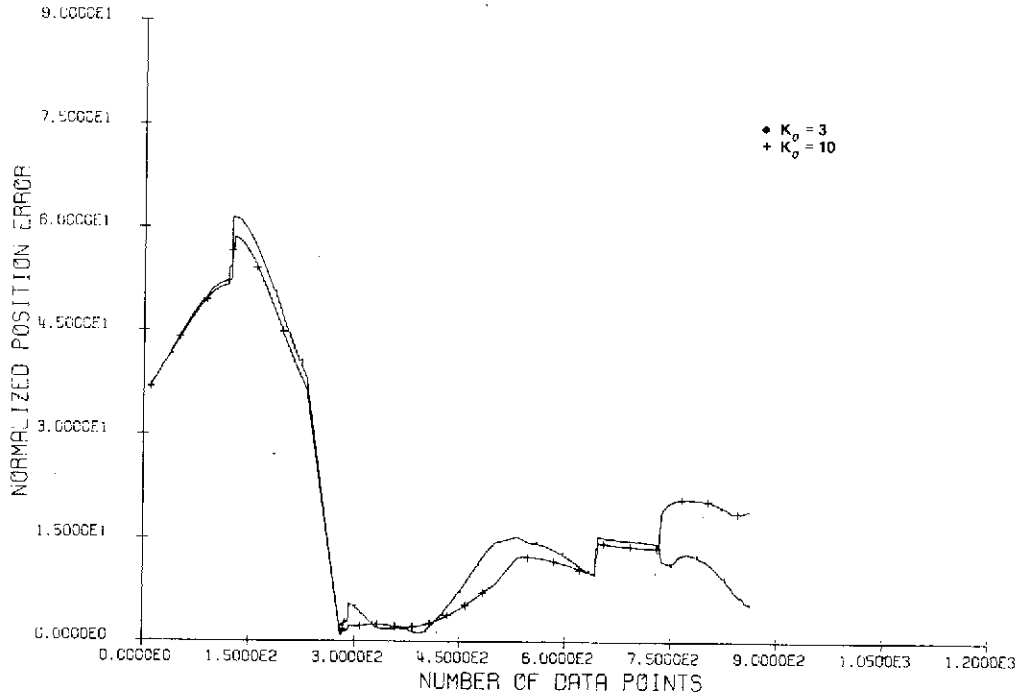

(a)

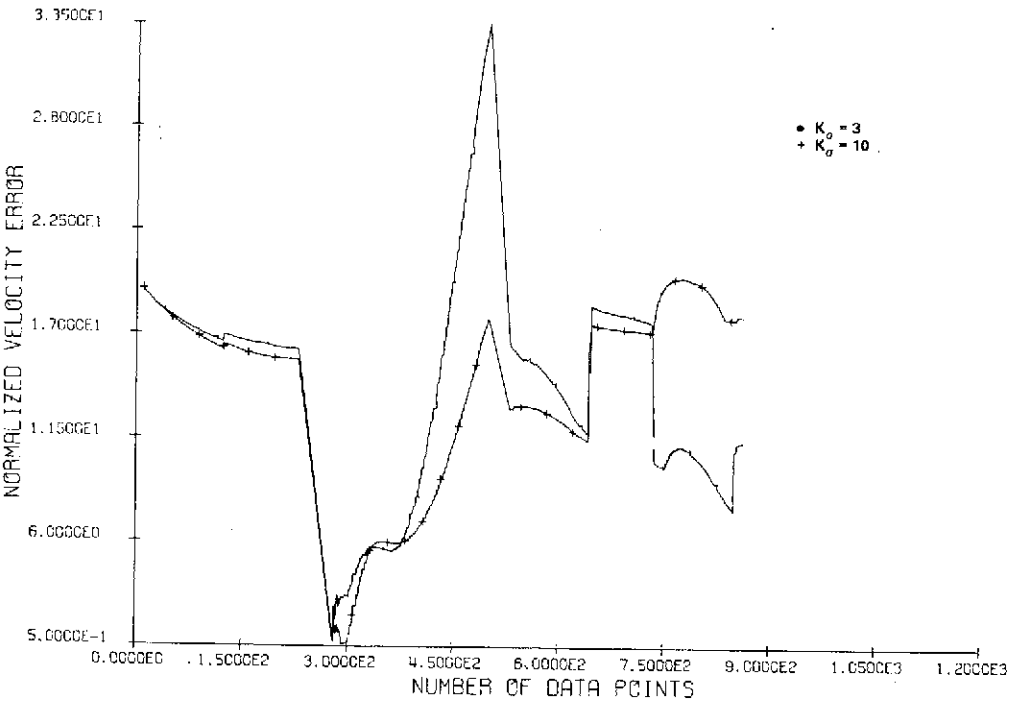

(b)

Figure 23. Comparison of Filter Errors (ERTS-1)

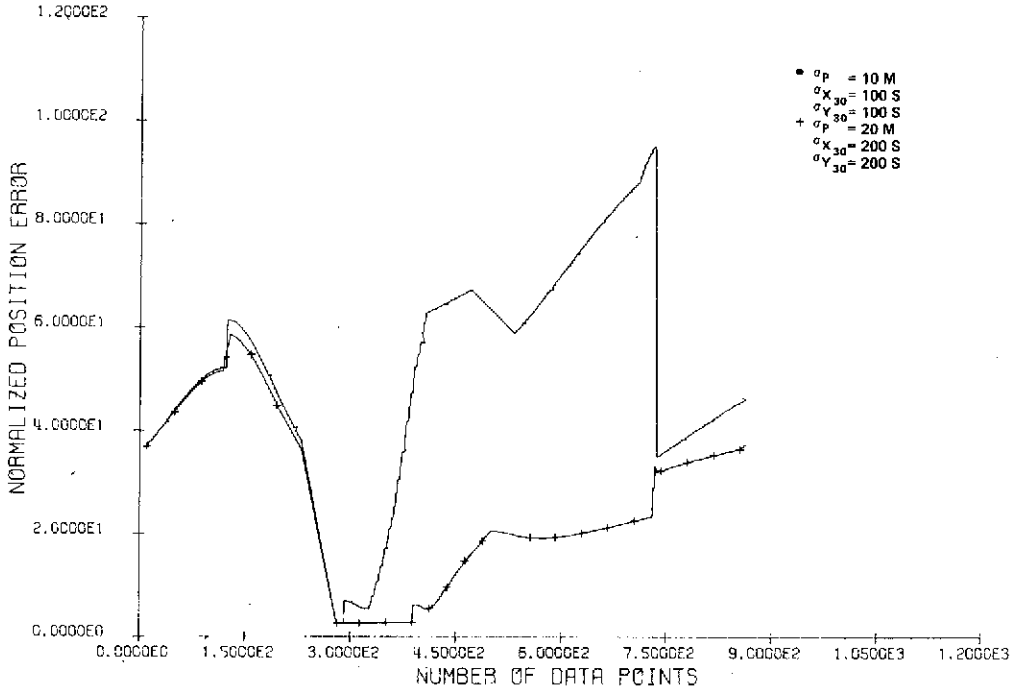

(a)

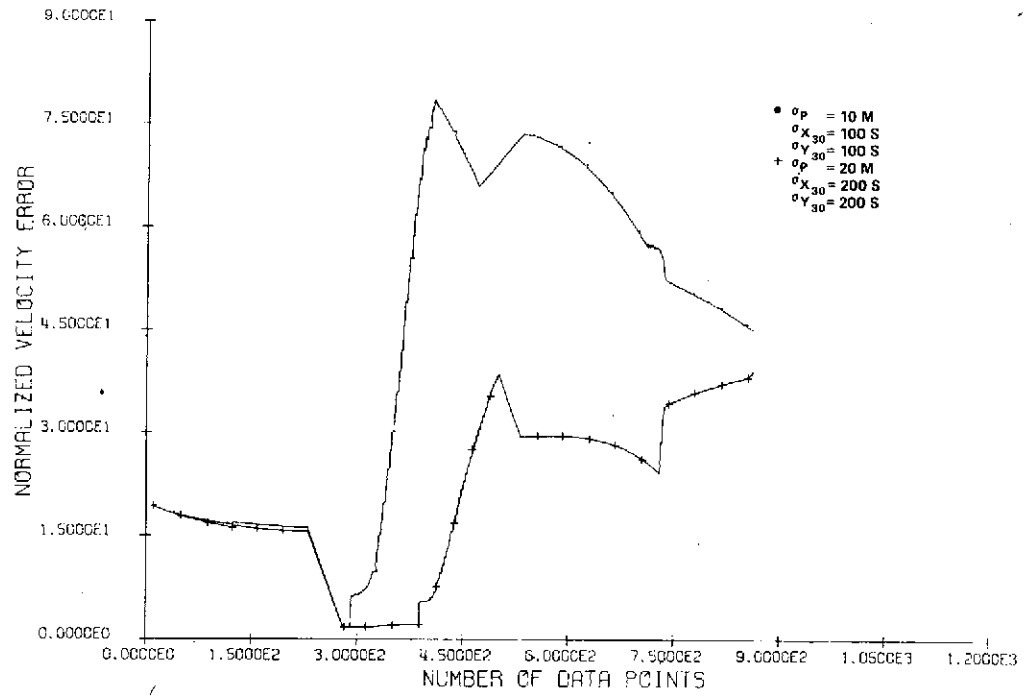

(b)

Figure 24. Comparison of Filter Errors (ERTS-1)

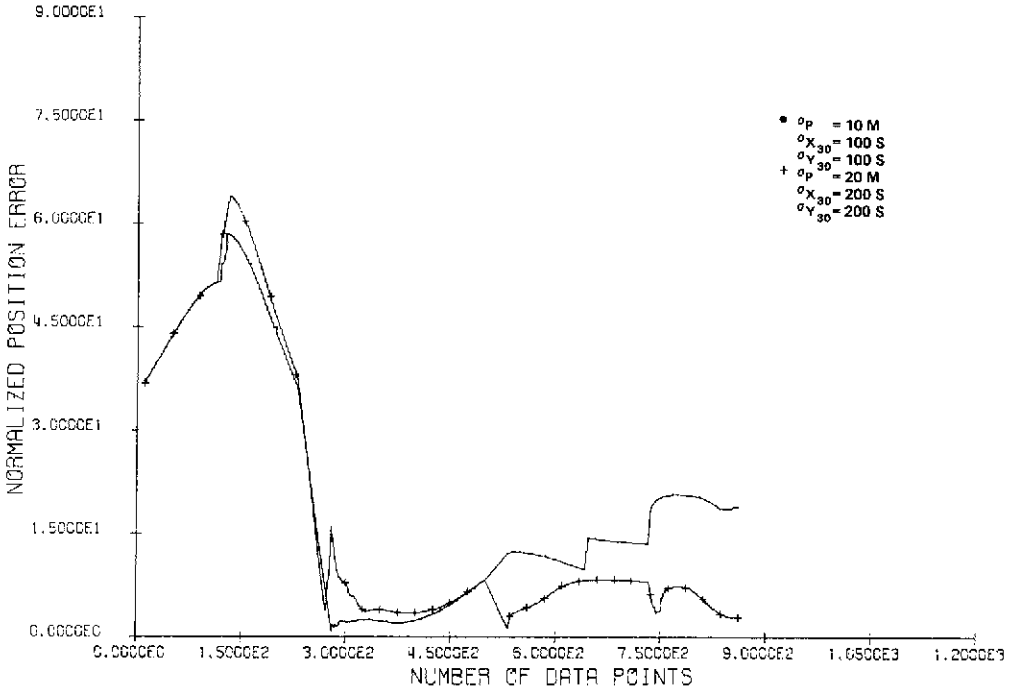

(a)

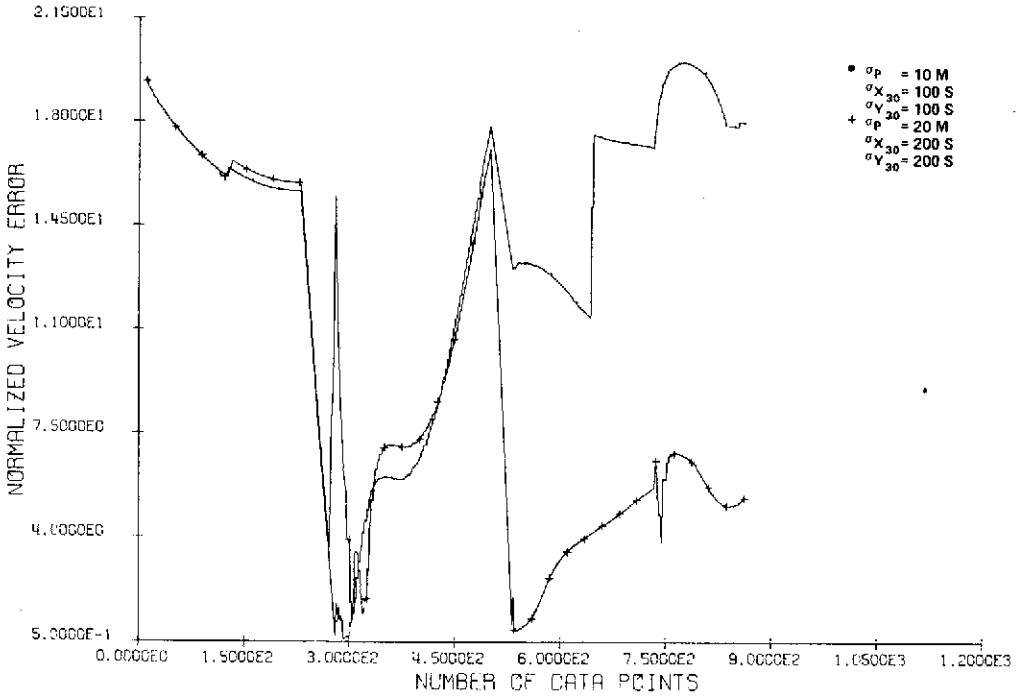

(b)

Figure 25. Comparison of Filter Errors (ERTS-1)

Table 1

Initial Covariance Matrices For RAE-B

P_{0_1}

0.2876E0	.2284E0	- .7631E0	.1207E-3	.8619E-4	-.2703E-3
	.2668E0	- .5675E0	.9615E-4	.1102E-3	-.2144E-3
		0.2061E1	-.3191E-3	-.2088E-3	.7275E-3
			.5539E-7	.4273E-7	-.1244E-6
				.5647E-7	-.9634E-7
					.2966E-6

P_{0_2}

.1348E0	.1165E0	- .3458E0	.4113E-4	.2771E-4	-.8272E-4
	.1508E0	- .2803E0	.3513E-4	.4302E-4	-.6686E-4
		.9234E0	-.1104E-3	-.6202E-4	.2222E-3
			.1631E-7	.1111E-7	-.3062E-7
				.1801E-7	-.2065E-7
					.6980E-7

P_{0_3}

1.	0.	0.	0.	0.	0.
	1.	0.	0.	0.	0.
		1.	0.	0.	0.
			1.E-4	0.	0.
				1.E-4	0.
					1.E-4

P_{0_4}

0.1	0.	0.	0.	0.	0.
	0.1	0.	0.	0.	0.
		0.1	0.	0.	0.
			1.E-6	0.	0.
				1.E-6	0.
					1.E-6

Table 2

Initial Covariance Matrix For IMP-J

P_{0_i}

.8891E0	-.5432E0	.9765E-1	.2865E-2	-.4460E-3	.8015E-6
	.2935E0	-.6129E-1	-.1445E-2	.4413E-3	-.1972E-3
		.9042E0	.2204E-3	.3102E-3	.3078E-2
			.2804E-2	.2736E-3	-.6640E-4
				.1986E-3	.6082E-3
					.2693E-2

Table 3

Initial Covariance Matrix For ERTS-1

.1817E-2	.2447E-3	.4235E-3	-.3340E-5	-.7459E-6	-.4287E-6
	.2877E-3	-.2601E-3	-.4989E-6	-.2645E-6	-.4263E-6
		.5127E-3	-.7031E-6	.3132E-7	.3739E-6
			.6177E-8	.1408E-8	.8776E-9
				.4132E-9	.4116E-9
					.6443E-9

VII

CONCLUSIONS AND RECOMMENDATIONS

Results show that the application of sequential filtering theory to orbit determination with the kind of data available today presents many problems. The precision reached, although in some cases comparable with that obtained in an iterative batch process (DC), is almost always lower.

The observations have to fulfill some necessary conditions for successful application of the filtering theory to this field, and this condition seems to be more strict than those required for a batch process. In this case the problem of estimation of the state is completely separated from that of estimation of the uncertainties of that state. In the sequential process these two problems are totally coupled so that the real number of parameters to be estimated is bigger in this case. The necessary condition that the observations have to accomplish is to restore the deterioration suffered by the state and its covariance matrix between observations. With an observation rate lower than this, the filter may diverge and only with a higher rate than that minimum one, may the estimation of the state improve. That minimum rate depends on the orbit type and observation type.

With these conditions accomplished, and with an initial covariance matrix perhaps improved by simulating, it seems feasible to use the filtering theory as an early orbit determination system in which raw data are used. In this work only the USB data used for ERTS-1 were raw. The improvement of the estimation by using raw data instead of smooth data has not been evaluated. Nevertheless, since in every smoothing process some information is lost, the results are going to be improved if this information is retained.

The potential recovery capability of the MJF has not been tested in this study since the possibility of doing so with the data used in this work seemed dim. The errors in the estimation of the state make the values obtained for the unmodeled accelerations completely unworthy. If the filter does not track the state correctly, this means that the unmodeled accelerations are not being tracked either, since the two problems are totally correlated. Potential recovery would require a much better tracking system, with almost continuous coverage.

The assumption of white noise for the observation noise is not real in most of the cases. This fact has more influence in the sequential processes than in the batch process. Another, more exact error model should be found in order that successful results in the high precision fast orbit determination problem can be realized.

VIII

REFERENCES

1. Jazwinski, A. H., "Stochastic Processes and Filtering Theory," Academic Press, New York, 1970.

2. Jazwinski, A. H., Hipkins, C., "Adaptive Estimation for Model Enhancement in Satellite Orbit Determination," Business and Technological Systems, Inc., BTS-TR-72-1 (Final Report), July 1972.

3. Argentiero, P., "Adaptive Filtering with Correlated State Noise," GSFC X-JJ1-72-394, October 1972.

4. Jazwinski, A. H., Hipkins, C., "J-Adaptive Estimation with Estimated Noise Statistics," Business and Technological Systems, Inc., BTS-TR-73-5 (Final Report), November 1973.

5. Chul Young Choe, "Nonlinear Estimation Theory Applied to Orbit Determination," Applied Mechanics Research Laboratory, Report No. AMRL-1038, The University of Texas at Austin, May 1972.